

PYRAMIDKV: DYNAMIC KV CACHE COMPRESSION BASED ON PYRAMIDAL INFORMATION FUNNELING

Anonymous authors

Paper under double-blind review

ABSTRACT

In this study, we investigate whether attention-based information flow inside large language models (LLMs) is aggregated through noticeable patterns for long context processing. Our observations reveal that LLMs aggregate information through **Pyramidal** Information Funneling where attention is scattering widely in lower layers, progressively consolidating within specific contexts, and ultimately focusing on critical tokens (a.k.a massive activation or attention sink) in higher layers. Motivated by these insights, we developed PyramidKV, a novel and effective KV cache compression method. This approach dynamically adjusts the KV cache size across different layers, allocating more cache in lower layers and less in higher ones, diverging from traditional methods that maintain a uniform KV cache size. Our experimental evaluations, utilizing the LongBench benchmark, show that PyramidKV matches the performance of models with a full KV cache while retaining only 12% of the KV cache, thus significantly reducing memory usage. In scenarios emphasizing memory efficiency, where only 0.7% of the KV cache is maintained, PyramidKV surpasses other KV cache compression techniques, achieving up to a 20.5 absolute accuracy improvement on TREC dataset. In the Needle-in-a-Haystack experiment, PyramidKV outperforms competing methods in maintaining long-context comprehension in LLMs; notably, retaining just 128 KV cache entries enables the LLAMA-3-70B model to achieve 100.0 Acc. performance, matching that of a full KV cache.

1 INTRODUCTION

Large language models (LLMs) (Achiam et al., 2023; Touvron et al., 2023a;b; Jiang et al., 2023) are integral to various natural language processing applications, including dialogue systems (Chiang et al., 2023), document summarization (Fabri et al., 2019a), and code completion (Roziere et al., 2023). These models have recently been scaled up to handle long contexts (Fu et al., 2024; Ding et al., 2024; Zhu et al., 2023; Chen et al., 2023), with GPT-4 processing up to 128K tokens and Gemini-pro-1.5 handling 1M tokens. However, scaling LLMs to extremely long contexts naturally leads to a significant delay due to the quadratic computation of attention over long contexts. A common solution to mitigate such inference delays involves caching the key and value states (KV) of previous tokens (Waddington et al., 2013), with the trade-off of requiring extensive GPU memory storage. For instance, maintaining a KV cache for 100K tokens in LLaMA-2 7B requires over 50GB of memory, while a 2K context requires less than 1GB of memory (Wu et al., 2024).

To tackle these memory constraints, recent studies have explored the optimization of KV caching, including approaches such as low-rank decomposition of the KV cache (Dong et al., 2024) or pruning non-essential KV cache (Zhang et al., 2024; Li et al., 2024; Ge et al., 2023). Notably, it has been shown that maintaining merely 20% of the KV cache can preserve a substantial level of performance (Zhang et al., 2024). Moreover, extreme compression of the KV cache for tasks of longer contexts (e.g., retrieval augmented generation or RAG for short) can drastically improve efficiency and further reduce resource use. However, questions about the universal applicability of these strategies across all layers of an LLM remain open. (1) *Are these KV cache strategies applicable to all layers?* (2) *Is it computationally efficient to use the same KV cache size across layers as previous studies have done?* These considerations suggest a need for an in-depth, more nuanced understanding of KV cache optimization in LLMs.

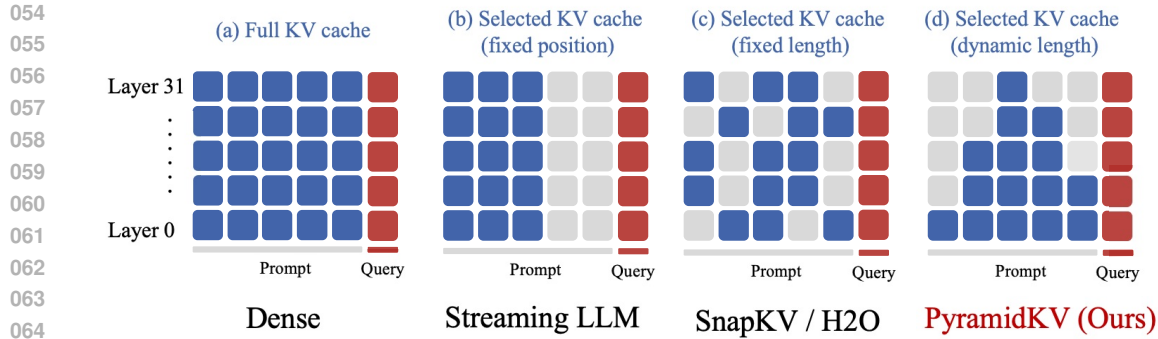


Figure 1: Illustration of PyramidKV compared with existing KV cache compression methods. (a) Full KV has all tokens stored in the KV cache in each layer; cache size increases as the input length increases. (b) StreamingLLM (Xiao et al., 2023) only keeps few initial tokens with a fixed cache size in each layer. (c) SnapKV (Li et al., 2024) and H2O (Zhang et al., 2024) keep a fixed cache size across Transformer layers, and their selection is based on the attention score. (d) PyramidKV maintains pyramid-like cache sizes, allocating more cache budget to lower layers and less to higher layers. This approach to KV cache selection better aligns with the increasing attention sparsity observed in multi-layer Transformers (§3).

To examine these questions, we aim to systematically investigate the design principles of the KV cache compression across different layers, specifically tailored to the behaviors of the attention mechanism. We first investigate how information flow is aggregated via attention mechanisms across different layers in multi-document question answering (QA), a classic task involving long contexts. Our analysis identifies a notable transition of attention distribution from a broad coverage of global contexts to a narrow focus of local tokens over layers in LLMs. This pattern suggests an aggregated information flow where information is initially gathered broadly and subsequently narrowed down to key tokens, epitomizing the massive attention phenomenon. Our findings provide unique insights beyond the previously documented “massive activation” (Sun et al., 2024) that very few activations exhibit significantly larger values than others when calculating multi-head attention in LLMs and “attention sink” (Xiao et al., 2023) that keeping the KV of initial tokens will largely recover the performance of window attention.

Building on these insights on how information flows are aggregated through a pyramid pattern, we design a novel and effective KV cache pruning approach that mirrors the geometric shape, named PyramidKV. As shown in Figure 1, unlike the fixed-and-same length KV cache pruning common in prior works (Zhang et al., 2024; Ge et al., 2023; Li et al., 2024), PyramidKV allocates more KV cache to the lower layers where information is more dispersed and each KV holds less information while reducing the KV cache in higher layers where information becomes concentrated in fewer key tokens. To the best of our knowledge, PyramidKV is the first KV cache compression method with varied cache retention across layers, tailoring cache amounts to the informational needs of each layer and paving the way for future research.

We conducted comprehensive experiments on LongBench (Bai et al., 2023) using 17 datasets across various tasks and domains with three backbone models (LLaMa-3-8B-Instruct, LLaMa-3-70B-Instruct and Mistral-7B (Jiang et al., 2023)). The results show that PyramidKV preserves performance using just 12.0% of the KV cache (KV Cache size = 2048) on the LongBench benchmark and significantly outperforms other methods in extreme conditions, retaining only 0.7% of the KV cache. Moreover, PyramidKV outperforms baseline models (H2O (Zhang et al., 2024), SnapKV (Li et al., 2024), StreamingLLM (Xiao et al., 2023)) across all tested cache sizes (64, 96, 128, 256), with its advantages most pronounced at smaller cache sizes. In the Needle In A Haystack experiment, PyramidKV effectively maintains the long-context comprehension in LLMs, outperforming than competing methods. Remarkably, with PyramidKV, retaining only 128 KV cache entries allows the LLaMa-3-70B-Instruct model to achieve 100.0 Acc. performance, matching the performance of a full KV cache.

2 RELATED WORK

Interpretation of LLMs Prior research has shown that attention matrices in LLMs are typically sparse (Chen et al., 2024a; Xiao et al., 2023; Zhang et al., 2024), focusing disproportionately on a few tokens. For instance, Xiao et al. (2023) identified an “attention sink” phenomenon, where maintaining the Key and Value (KV) states of the first few tokens can substantially restore the performance of windowed attention, despite these tokens not being semantically crucial. Similarly, Sun et al. (2024) identified a “massive activations” pattern, where a minority of activations show significantly larger values than others within LLMs. Interestingly, these values remain relatively constant across different inputs and act as critical bias terms in the model.

Further explorations in this field reveal distinct patterns across various attention heads and layers. Li et al. (2024) observed that certain attention heads consistently target specific prompt attention features during decoding. Additionally, Wang et al. (2023) discovered that in In-Context Learning scenarios, label words in demonstration examples serve as semantic anchors. In the lower layers of an LLM, shallow semantic information coalesces around these label words, which subsequently guide the LLMs’ final output predictions by serving as reference points. Recently, Wu et al. (2024) revealed that a special type of attention head, the so-called retrieval head, is largely responsible for retrieving information. Inspired by these findings that the attention mechanism exhibits varying behaviors across different layers, we discovered that “Massive Activation” does not consistently manifest across all layers in long context sequences; instead, it predominantly occurs in the upper layers. Additionally, we identified a novel trend of information aggregation specific to long-context inputs, which will be further explained in §3.

KV Cache Compression There has been a growing interest in addressing LLMs’ memory constraints on processing long context inputs. FastGen (Ge et al., 2023) introduces an adaptive KV cache management strategy that optimizes memory use by tailoring retention tactics to the specific nature of attention heads. This method involves evicting long-range contexts from heads that prioritize local interactions, discarding non-special tokens from heads focused on special tokens, and maintaining a standard KV cache for heads that engage broadly across tokens. SnapKV (Li et al., 2024) improves efficiency by compressing KV caches via selecting/clustering significant KV positions based on their attention scores. Heavy Hitter Oracle (H2O) (Zhang et al., 2024) implements a dynamic eviction policy that effectively balances the retention of recent and historically significant tokens, optimizing memory usage while preserving essential information. StreamingLLM (Xiao et al., 2023) enables LLMs trained on finite attention windows to handle infinite sequence lengths without fine-tuning, thus expanding the models’ applicability to broader contexts. LM-Infinite (Han et al., 2023) allows LLMs pre-trained with 2K or 4K-long segments to generalize to up to 200M length inputs while retaining perplexity without parameter updates.

While these approaches have significantly advanced the efficient management of memory for LLMs, they generally apply a fixed KV cache size across all layers. In contrast, our investigations into the attention mechanisms across different layers of LLMs reveal that the attention patterns vary from layer to layer, making a one-size-fits-all approach to KV cache management suboptimal. In response to this inefficiency, we propose a novel KV cache compression method, called PyramidKV that allocates different KV cache budgets across different layers, tailored to the unique demands and operational logic of each layer’s attention mechanism. This layer-specific strategy takes a significant step toward balancing both memory efficiency and model performance, addressing a key limitation in existing methodologies.

3 PYRAMIDAL INFORMATION FUNNELING

To systematically understand the attention mechanism over layers in LLMs for long-context inputs, we conduct a fine-grained study focusing on the multi-document question answering (QA) task. The model is presented with multiple interrelated documents and prompted to generate an answer for the given query. The main target is to investigate how the model aggregates dispersed information within these retrieved documents for accurate responses.

In particular, we focus on our analysis of the LLaMa (Touvron et al., 2023a;b) and visualize the distribution and behavior of attention scores over layers. To assess the distinct behaviors of each

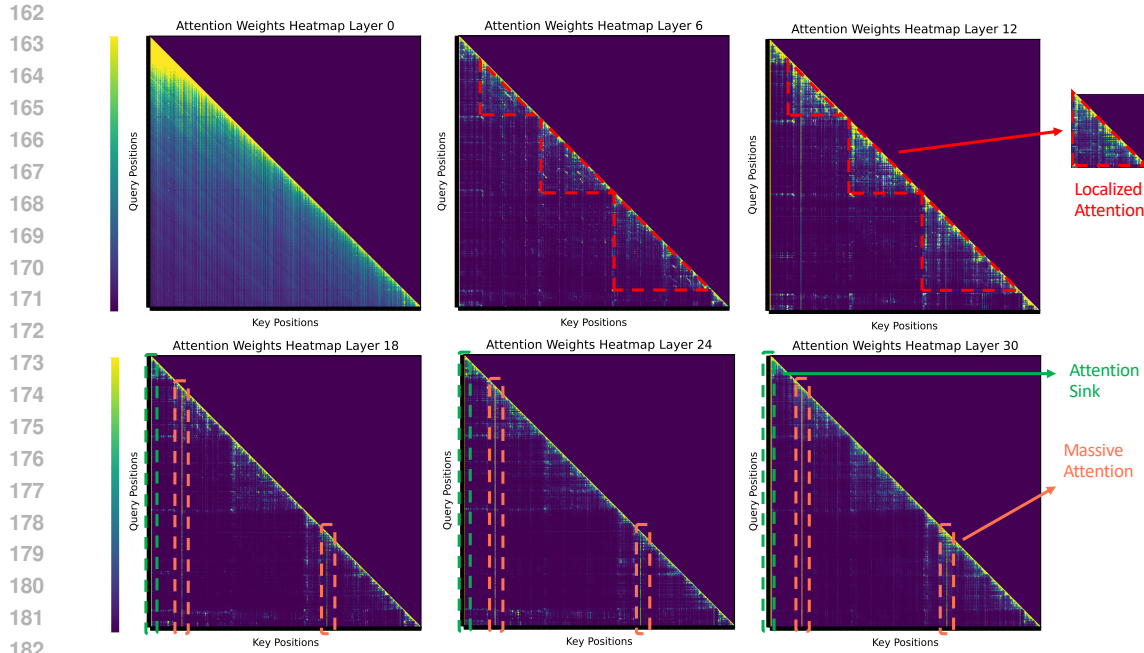


Figure 2: Attention patterns of retrieval-augmented generation across layers in LLaMa (Touvron et al., 2023a;b) reveal that in the lower layers, the model exhibits a broad-spectrum mode of attention, distributing attention scores uniformly across all content. In the middle layers, attention becomes more localized within each document, indicating refined information aggregation (dotted red triangular shapes in layers 6 and 10). This culminates in the upper layers, where “massive attention” focuses on a few key tokens (concentrated attention bars after layer 18), efficiently extracting essential information for answers.

multi-head self-attention layer, we compute the average attention from all heads within each layer. Figure 2 shows the attention patterns of one QA example over six different layers (i.e., 0, 6, 12, 18, 24, and 30).

We identify an approximately uniform distribution of attention scores from the lower layers (e.g., the 0th layer). This suggests that the model operates in a broad-spectrum mode at the lower layers, aggregating information globally from all available content without prioritizing its attention on specific input segments. Notably, a distinct transition to a more localized attention pattern within each document emerges, as the model progresses to encode information at the middle layers (6th to 18th layers). In this phase, attention is predominantly directed towards tokens within the same document, suggesting a more refined aggregation of information within individual contexts.

This trend continues and intensifies in the upper layers (from the 24th to the 30th layer), where we observed the emergence of ‘massive attention’ phenomena. In these layers, the attention mechanism concentrates overwhelmingly on a few key tokens. This pattern of attention allocation, where extremely high attention scores are registered, signifies that the model has aggregated the essential information into these focal tokens. Such behavior underscores a sophisticated mechanism by which LLMs manage and streamline complex and voluminous information, culminating in the efficient extraction of the most pertinent data points necessary for generating accurate answers.

4 PYRAMIDKV

4.1 PRELIMINARIES AND PROBLEM FORMULATION

In an autoregressive transformer-based LLM, the generation of the i -th token requires that the attention module computes the query, key, and value vectors for all previous $i - 1$ tokens. To speed

up the inference process and avoid duplicate computations, the key and value matrices are typically stored in the GPU memory. While the KV cache enhances inference speed and reduces redundant computations, it can consume significant memory when dealing with long input contexts. To optimize memory usage, a strategy called KV cache compression is proposed (Zhang et al., 2024; Xiao et al., 2023; Li et al., 2024), which involves retaining only a minimal amount of KV cache while preserving as much information as possible.

In a language model with m transformer layers, we denote the key and value matrices in the l -th attention layer respectively as $\mathbf{K}^l, \mathbf{V}^l \in \mathbb{R}^{n \times d}, \forall l \in [0, m - 1]$ when encoding a sequence of n tokens. The goal of KV cache compression is to seek two sub-matrices $\mathbf{K}_s^l, \mathbf{V}_s^l \in \mathbb{R}^{k^l \times d}$ from the full matrices \mathbf{K}^l and \mathbf{V}^l , given a cache budget $k^l < n$ for each layer $l \in [0, m - 1]$ while maximizing performance preservation. That is, a language model with KV cache compression only uses \mathbf{K}_s^l and \mathbf{V}_s^l in the GPU memory for inference on a dataset \mathcal{D} , and obtains a similar result to a full model according to an evaluation scoring metric, i.e., $\text{score}(\mathbf{K}^l, \mathbf{V}^l, \mathcal{D}) \approx \text{score}(\mathbf{K}_s^l, \mathbf{V}_s^l, \mathcal{D})$.

4.2 PROPOSED METHOD

In this section, we introduce our method, PyramidKV, based on the pyramidal information funneling observed across different layers in §3. PyramidKV consists of two steps: (1) Dynamically allocating different KV cache sizes/budgets across different layers (§4.2.1); and (2) Selecting important KV vectors in each attention head for caching (§4.2.2).

4.2.1 KV CACHE SIZE/BUDGET ALLOCATION

Previous work on KV cache compression (Li et al., 2024; Zhang et al., 2024; Xiao et al., 2023) often allocates a fixed KV cache size across LLM layers. However, as our analysis in §3 demonstrates, attention patterns are not identical across different layers. Particularly dense attention is observed in the lower layers, and sparse attention in higher layers. Therefore, using a fixed KV cache size across different layers may lead to suboptimal performance. These approaches may retain many unimportant tokens in the higher layers of sparser attentions while potentially overlooking many crucial tokens in the lower layers of denser attentions.

Thus, we propose to increase compression efficiency by dynamically allocating the cache budgets across layers to reflect the aggregated information flow based on attention patterns. Specifically, PyramidKV allocates more KV cache to the lower layers where information is more dispersed and each KV state contains less information, while reducing the KV cache in higher layers where information becomes concentrated in a few key tokens.

Following the common practice in KV cache compression (Li et al., 2024; Xiao et al., 2023), we first retain the KV cache for the last α tokens of the input across all layers, as these tokens have been shown to contain the most immediate task-related information, where α is a hyperparameter, controlling the number of last few tokens being included in the KV cache. For simplicity, we call these tokens “*instruction tokens*”, which is also referred to as “*local window*” in previous literature (Zhang et al., 2024; Li et al., 2024; Xiao et al., 2023).

Subsequently, given the remaining total cache budget $k^{\text{total}} = \sum_{l \in [0, m-1]} k^l$ that can be used over all transformer layers (noted as m), we first determine the cache sizes for the top and bottom layers, and use an arithmetic sequence to compute the cache sizes for the intermediate layers to form the pyramidal shape. The key intuition is to follow the attention pattern in aggregated information flow, reflecting a monotonically decreasing pattern of important tokens for attention from lower layers to upper layers. We allocate $k^{m-1} = k^{\text{total}} / (\beta \cdot m)$ for the top layer and $k^0 = (2 \cdot k^{\text{total}}) / m - k^{m-1}$ for the bottom layer, where β is a hyperparameter to adjust the pyramid’s shape. The hyperparameter β is still required to determine the top layer. Once the top layer is identified, the budget of the bottom layer can be calculated by summing the budgets across all layers and equating this sum to the total budget. Once the cache sizes of the bottom and top layers are determined, the cache sizes for all intermediate layers are set according to an arithmetic sequence, defined as

$$k^l = k^0 - \frac{k^0 - k^{m-1}}{m - 1} \times l. \quad (1)$$

4.2.2 KV CACHE SELECTION

Once the KV cache budget is determined for each layer, our method needs to select specific KV states for caching within each layer in LLMs. As described in the previous section, the KV cache of the last α tokens, referred to as instruction tokens, are retained across all layers. Following SnapKV (Li et al., 2024), the selection of the remaining tokens is then guided by the attention scores derived from these instruction tokens—tokens receiving higher attention scores are deemed more relevant to the generation process and are thus their KV states are prioritized for retention in the GPU cache.

In a typical LLM, the attention mechanism in each head h is calculated using the formula:

$$\mathbf{A}^h = \text{softmax}(\mathbf{Q}^h \cdot (\mathbf{K}^h)^\top / \sqrt{d_k}), \quad (2)$$

where d_k denotes the dimension of the key vectors. Following (Li et al., 2024), we utilize a pooling layer at \mathbf{A}^h to avoid the risk of being misled by some massive activation scores.

To quantify the importance of each token during the generation process, we measure the level of attention each token receives from the instruction tokens, and use this measurement to select important tokens for KV caching. Specifically, we compute the score of selecting i -th token for retention in the KV cache as s_i^h in each attention head h by:

$$s_i^h = \sum_{j \in [n-\alpha, n]} \mathbf{A}_{ij}^h \quad (3)$$

where $[n - \alpha, n]$ is the range of the instruction tokens. In each layer l and for each head h , the top k^l tokens with the highest scores are selected, and their respective KV caches are retained. All other KV caches are discarded and will not be utilized in any subsequent computations throughout the generation process.

5 EXPERIMENT

We conduct comprehensive experiments to evaluate the effectiveness of PyramidKV on performance preserving and memory reduction. First, we introduce the experiment setup (§5.1) as backbone LLMs (§5.1.1), the evaluation datasets (§5.1.2), and the baselines in comparison (§5.1.3). Next, we report the performance in a memory-oriented scenario and a performance-oriented scenario experiments in §5.2. We also do some insight experiment (§5.3) to test if the model can preserve the performance on long-context inputs on the Needle-in-the-haystack experiment (§5.3.1). Finally, we discuss the trade-off between memory, time, and performance in §5.3.2.

5.1 EXPERIMENT SETUP

We maintain a fixed constant KV cache size for each layer for the baseline methods. In contrast, PyramidKV employs varying KV cache sizes across different layers. To ensure a fair comparison, we adjusted the average KV cache size in PyramidKV to match that of the baseline models, to keep the total memory consumption of all methods the same. In our experiment, we set $\beta = 20$ and $\alpha = 8$. We use the same prompt for each dataset in all the experiments.

5.1.1 BACKBONE LLMs

We compare PyramidKV against baselines using state-of-the-art open-sourced LLMs, namely LLaMa-3-8B-Instruct, Mistral-7B-Instruct (Jiang et al., 2023) and LLaMa-3-70B-Instruct. Testing examples are evaluated in a generative format, with answers generated by greedy decoding across all tasks to ensure a fair comparison.

5.1.2 DATASETS

We use LongBench (Bai et al., 2023) to assess the performance of PyramidKV on tasks involving long-context inputs. LongBench is a meticulously designed benchmark suite that tests the capabilities

of language models in handling extended documents and complex information sequences. This benchmark was created for comprehensive multi-task evaluation of long context inputs. It includes 17 datasets covering tasks such as single-document QA (Kočíšký et al., 2018; Dasigi et al., 2021), multi-document QA (Yang et al., 2018; Ho et al., 2020), summarization (Huang et al., 2021; Zhong et al., 2021; Fabbri et al., 2019b), few-shot learning (Li and Roth, 2002; Gliwa et al., 2019; Joshi et al., 2017), synthetic, and code generation (Guo et al., 2023; Liu et al., 2023b). The datasets feature an average input length ranging from 1,235 to 18,409 tokens (detailed average lengths can be found in Table 1), necessitating substantial memory for KV cache management. For all these tasks, we adhered to the standard metrics recommended by LongBench (Bai et al., 2023) (i.e., F1 for QA, Rouge-L for summarization, Acc. for synthetic and Edit Sim. for code generation.) We refer readers to more details at Appendix E.

5.1.3 BASELINES

We compare PyramidKV with three baselines, all of which keep the same KV cache size across different layers, with different strategies for KV cache selection.

StreamingLLM (SLM) (Xiao et al., 2023) is an efficient framework that enables LLMs trained with a finite length attention window to generalize to infinite sequence length without any fine-tuning. They propose StreamingLLM based on the attention sink phenomenon that keeping the KV of the first few tokens will largely recover the performance of window attention. StreamingLLM is a competitive method to solve long-context tasks. In our experiments, to be consistent with other methods, we simply keep the KV cache of the last α tokens and the first $k - \alpha$ tokens, as suggested in the paper.

Heavy Hitter Oracle (H2O) (Zhang et al., 2024) is a KV cache compression policy that dynamically retains a balance of recent and Heavy Hitter (H2) tokens. H2O keeps a fixed cache size of the Key and Value matrix across Transformer layers. The selection process for the KV cache is driven by attention scores, specifically utilizing the average attention scores from all queries across all tokens to guide the selection.

SnapKV (SKV) (Li et al., 2024) automatically compresses KV caches by selecting clustered important tokens for each attention head. This method discerns the attention patterns of the Key and Value matrices using a localized observation window positioned at the end of the prompts. However, unlike H2O, SnapKV employs a more nuanced clustering algorithm that includes a pooling layer. Additionally, SnapKV captures attention signals using patterns from a localized window (Instruction Tokens), rather than aggregating attention across all queries, allowing for more targeted and efficient compression.

FullKV (FKV) caches all keys and values for each input token in each layer. All methods are compared to the FullKV simultaneously.

5.2 MAIN RESULTS

The evaluation results from LongBench (Bai et al., 2023) are shown in Table 1 and Figure 3. In Figure 3, we report the average score across datasets for 64, 96, 128, and 256 case sizes. In Table 1, we report the results for two different KV cache sizes with 64 and 2048. These two sizes represent two distinct operational scenarios—the memory-efficient scenario and the performance-preserving scenario, respectively for a trade-off between memory and model performance. In Appendix M, we report the results of KV cache sizes with 64, 96, 128 and 2048.

Overall, PyramidKV preserves the performance with only 12% of the KV cache and it consistently surpasses other method across a range of KV cache sizes and different backbone models, with its performance advantages becoming particularly pronounced in memory-constrained environments where only about 0.8% of the KV cache from the prompt is retained. Upon examining specific tasks, PyramidKV demonstrates a notably superior performance on the TREC task, a few-shot question answering challenge. This suggests that the model effectively aggregates information from the few-shot examples, highlighting the potential for further investigation into in-context learning tasks.

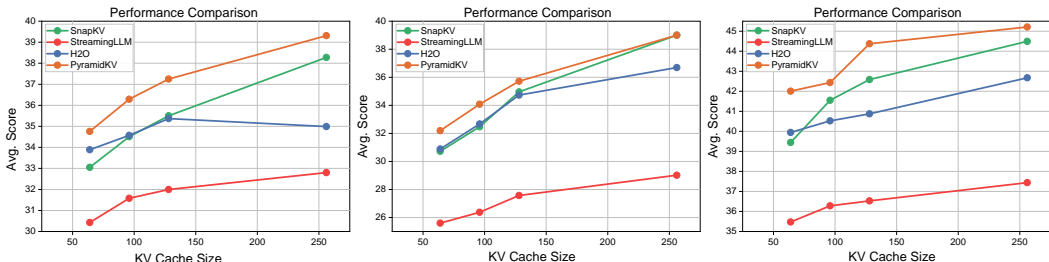


Figure 3: The evaluation results from LongBench (Bai et al., 2023) across 64, 96, 128 and 256 cache sizes at LLaMa-3-8B-Instruct (Left), Mistral-7B-Instruct (Middle) and LLaMa-3-70B-Instruct (Right). The evaluation metrics are the average score of LongBench across datasets. PyramidKV outperforms H2O (Zhang et al., 2024), SnapKV (Li et al., 2024) and StreamingLLM (Xiao et al., 2023), especially in small KV cache sizes.

Method	Single-Document QA			Multi-Document QA		Summarization			Few-shot Learning		Synthetic		Code		Avg.		
	NrivQA	Qasper	MF-en	HotpotQA	2WikiMQA	Musique	GovReport	QMSum	MultiNews	TREC	TriviaQA	SAMSum	PCount	Pre		Lcc	RB-P
LlaMa-3-8B-Instruct, KV Size = Full																	
FKV	25.70	29.75	41.12	45.55	35.87	22.35	25.63	23.03	26.21	73.00	90.56	41.88	4.67	69.25	58.05	50.77	41.46
LlaMa-3-8B-Instruct, KV Size = 64																	
SKV	19.86	9.09	27.89	37.34	28.35	18.17	15.86	20.80	16.41	38.50	85.92	36.32	5.22	69.00	51.78	48.38	33.05
H2O	20.80	11.34	27.03	37.25	30.01	17.94	18.29	21.49	19.13	38.00	84.70	37.76	5.63	69.33	53.44	50.15	33.89
SLM	17.44	8.68	22.25	35.37	31.51	15.97	15.46	20.06	14.64	38.00	72.33	29.10	5.42	69.50	46.14	45.09	30.43
Ours	21.13	14.18	30.26	35.12	23.76	16.17	18.33	21.65	19.23	58.00	88.31	37.07	5.23	69.50	52.61	45.74	34.76
LlaMa-3-8B-Instruct, KV Size = 2048																	
SKV	25.86	29.55	41.10	44.99	35.80	21.81	25.98	23.40	26.46	73.50	90.56	41.66	5.17	69.25	56.65	49.94	41.35
SLM	21.71	25.78	38.13	40.12	32.01	16.86	23.14	22.64	26.48	70.00	83.22	31.75	5.74	68.50	53.50	45.58	37.82
H2O	25.56	26.85	39.54	44.30	32.92	21.09	24.68	23.01	26.16	53.00	90.56	41.84	4.91	69.25	56.40	49.68	39.35
Ours	25.40	29.71	40.25	44.76	35.32	21.98	26.83	23.30	26.19	73.00	90.56	42.14	5.22	69.25	58.76	51.18	41.49
Mistral-7B-Instruct, KV Size = Full																	
FKV	26.90	33.07	49.20	43.02	27.33	18.78	32.91	24.21	26.99	71.00	86.23	42.65	2.75	86.98	56.96	54.52	42.71
Mistral-7B-Instruct, KV Size = 64																	
SKV	16.94	17.17	39.51	36.87	22.26	15.18	14.75	20.35	21.45	37.50	84.16	37.28	4.50	61.13	42.40	38.44	30.72
SLM	15.01	13.84	28.74	30.97	24.50	13.42	13.25	19.46	19.17	35.50	76.91	29.61	4.67	27.33	38.71	35.29	25.60
H2O	18.19	19.04	37.40	30.18	22.22	13.77	16.60	21.52	21.98	37.00	81.02	38.62	5.00	66.03	43.54	40.46	30.88
Ours	20.91	20.21	39.94	33.57	22.87	15.70	17.31	21.23	21.41	54.00	81.98	36.96	3.58	60.83	44.52	37.99	32.19
Mistral-7B-Instruct, KV Size = 2048																	
SKV	25.89	32.93	48.56	42.96	27.42	19.02	26.56	24.47	26.69	70.00	86.27	42.57	5.50	88.90	50.42	46.72	41.56
SLM	20.31	26.64	45.72	35.25	24.31	12.20	27.47	21.57	24.51	68.50	71.95	31.19	5.00	22.56	43.38	37.08	32.35
H2O	25.76	31.10	49.03	40.76	26.52	17.07	24.81	23.64	26.60	55.00	86.35	42.48	5.50	88.15	49.93	46.57	39.95
Ours	25.53	32.21	48.97	42.26	27.50	19.36	26.60	23.97	26.73	71.00	86.25	42.94	4.50	87.90	53.12	47.21	41.63
LlaMa-3-70B-Instruct, KV Size = Full																	
FKV	27.75	46.48	49.45	52.04	54.90	30.42	32.37	22.27	27.58	73.50	92.46	45.73	12.50	72.50	40.96	63.91	46.55
LlaMa-3-70B-Instruct, KV Size = 64																	
SKV	23.92	31.09	36.54	46.66	50.40	25.30	18.05	21.11	19.79	41.50	91.06	40.26	12.00	72.50	43.33	57.62	39.45
SLM	22.07	23.53	27.31	43.21	51.66	23.85	16.62	19.74	15.20	39.50	76.89	33.06	12.00	72.50	40.23	50.20	35.47
H2O	25.45	34.64	33.23	48.25	50.30	24.88	20.03	21.50	21.39	42.00	90.36	41.58	12.00	71.50	43.83	58.16	39.94
Ours	25.47	36.71	42.29	47.08	46.21	28.30	20.60	21.62	21.62	64.50	89.61	41.28	12.50	72.50	45.34	56.50	42.01
LlaMa-3-70B-Instruct, KV Size = 2048																	
SKV	26.73	45.18	47.91	52.00	55.24	30.48	28.76	22.35	27.31	72.50	92.38	45.58	12.00	72.50	41.52	69.27	46.36
SLM	26.69	41.01	35.97	46.55	52.98	25.71	27.81	20.81	27.16	69.00	91.55	44.02	12.00	72.00	41.44	68.73	43.96
H2O	27.67	46.51	49.54	51.49	53.85	29.97	28.57	22.79	27.53	59.00	92.63	45.94	12.00	72.50	41.39	63.90	45.33
Ours	27.22	46.19	48.72	51.62	54.56	31.11	29.76	22.50	27.27	73.50	91.88	45.47	12.00	72.50	41.36	69.12	46.55

Table 1: Performance comparison of PyramidKV (Ours) with SnapKV (SKV), H2O, StreamingLLM (SLM) and FullKV (FKV) on LongBench for LLaMa-3-8B-Instruct, Mistral-7B-Instruct and LLaMa-3-70B-Instruct. PyramidKV generally outperforms other KV Cache compression methods across various KV Cache sizes and LLMs. The performance strengths of PyramidKV are more evident in small KV Cache sizes (i.e. KV Size = 64). Bold text represents the best performance.

Notably, we initially observe the pyramidal attention patterns from the visualization analysis on the multi-document QA task (Figure 2), but the pyramid heuristic has demonstrated its effectiveness on a range of other LongBench tasks (e.g., single-document QA, In-Context Learning), suggesting its promising generalizability beyond multi-document QA.

The performance advantage of PyramidKV increases as the KV cache memory decreases. By focusing on optimizing budget allocation across layers, PyramidKV accurately allocates resources in memory-constrained scenarios, ensuring that retained information is effectively preserved to maintain model performance. Moreover, as in long bench results shown in Table 1, even in the performance-preserving scenario (i.e., KV cache size = 2048), PyramidKV still improves the performance over baseline methods and even outperforms the performance of FullKV.

Among the 16 datasets, the tasks where our proposed method performs slightly worse than the baseline are mostly saturated (e.g., HotpotQA, Musique, etc under the LLaMa-3-8B-Instruct setting with KV Size = 64, as shown in Table 1). In these cases, our method is only marginally inferior to the baseline and remains competitive. Conversely, on tasks with greater potential for improvement (e.g., Qasper, MF-en, TREC, TriviaQA, etc under the same setting), our method significantly outperforms the baseline. Consequently, the overall average performance of our method surpasses that of the baselines. Notably, these tasks include several In-Context Learning tasks (i.e., TREC), our method enjoys best performance gain at In-Context Learning tasks, where the method demonstrates the ability to leverage provided examples to adapt effectively. The importance of In-Context Learning tasks lies in their widespread use in real-world applications, where dynamic adaptation to new inputs is critical.

5.3 DISCUSSION AND INSIGHTS

5.3.1 PYRAMIDKV PRESERVES THE LONG-CONTEXT UNDERSTANDING ABILITY

We conduct the "Fact Retrieval Across Context Lengths" (Needle In A Haystack) experiment (Liu et al., 2023a; Fu et al., 2024), which is a dataset designed to test whether a model can find key information in long input sequences, to evaluate the in-context retrieval capabilities of LLMs when utilizing various KV cache compression methods. For this purpose, we employ **LLaMa-3-70B-Instruct** as our base, with context lengths extending up to 8k. We compared several KV cache compression techniques (PyramidKV, SnapKV (Li et al., 2024), and H2O (Zhang et al., 2024)) at cache sizes of **128** and full cache. The results, presented in Figure 4¹. The results demonstrate that with only 128 KV cache retained, PyramidKV effectively maintains the model’s ability to understand short contexts, and shows only modest degradation for longer contexts. In contrast, other KV cache compression methods significantly hinder the performance of LLMs. Notably, for the larger model (**LLaMa-3-70B-Instruct**), PyramidKV achieves 100.0 Acc. performance, matching the results of FullKV, thereby demonstrating its ability to preserve long-context comprehension with a substantially reduced KV cache. **We adopt the haystack setting of haystack formed from a long corpus for the Needle In A Haystack task as Wu et al. (2024).**

5.3.2 PYRAMIDKV SIGNIFICANTLY REDUCES MEMORY WITH LIMITED PERFORMANCE DROP

In this section, we study how sensitive the methods are with different sizes of KV cache. We report the KV cache memory reduction in Table 2. We evaluate the memory consumption of LLaMa-3-8B-Instruct. Specifically, we evaluate the memory consumption of all methods with a fixed batch size of 1, a sequence length of 8192, and model weights in fp16 format. We observe that PyramidKV substantially reduces the KV cache memory across different numbers of cache sizes.

We also present that the allocation strategy and score-based selection add minimal complexity in the inference phase compared to the computation required for next-token predictions as Appendix K.

6 CONCLUSION

In this study, we investigate the intrinsic attention patterns of Large Language Models (LLMs) when processing long context inputs. Our empirical analysis leads us to discover the existence of Pyramidal Information Funneling. Motivated by this discovery, we design a novel KV cache

¹Additional results with 64, 96 and 128 KV cache sizes with **LLaMa-3-8B-Instruct** at 8k context length, **LLaMa-3-70B-Instruct** at 8k context length, and **Mistral-7B-Instruct** (Jiang et al., 2023) at 32k context length are available in Appendix O

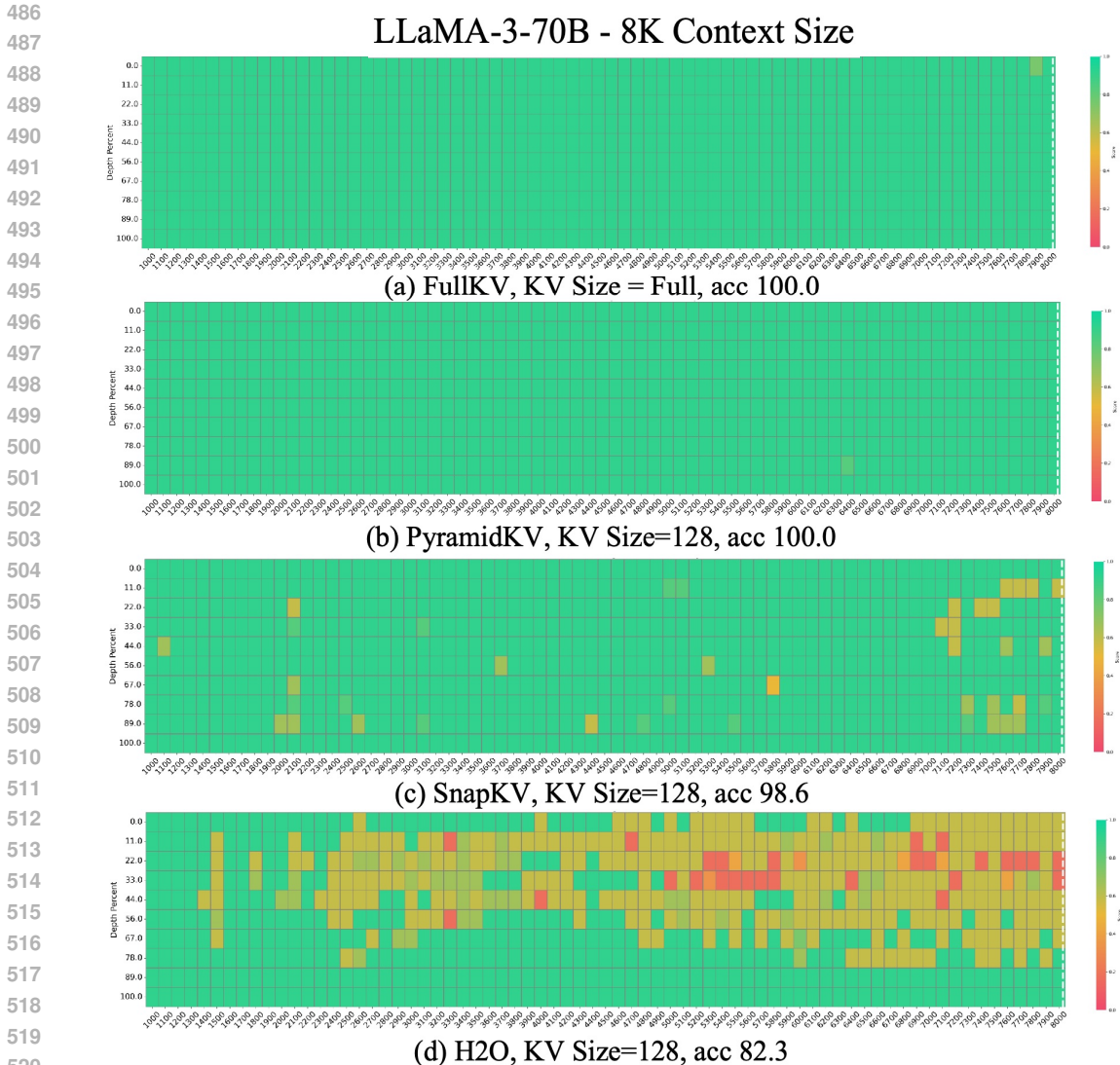


Figure 4: Results of the Fact Retrieval Across Context Lengths (“Needle In A HayStack”) test in **LlMa-3-70B-Instruct** with **8k** context size in **128** KV cache size. The vertical axis of the table represents the depth percentage, and the horizontal axis represents the token length.

cache size	Memory	Compression Ratio	QMSum	TREC	TriviaQA	PCount	Pre	Lcc
512	428M	6.3%	22.80	71.50	90.61	5.91	69.50	58.16
1024	856M	12.5%	22.55	71.50	90.61	5.91	69.50	58.16
2048	1712M	25.0%	22.55	72.00	90.56	5.58	69.25	56.79
Full	6848M	100.0%	23.30	73.00	90.56	5.22	69.25	58.76

Table 2: Memory reduction effect and benchmark result by using PyramidKV. We conducted a comparison of memory consumption between the Llama-3-8B-Instruct model utilizing the Full KV cache and the Llama-3-8B-Instruct model compressed with the PyramidKV.

compression approach PyramidKV that utilizes this information flow pattern. By leveraging the Pyramidal Information Funneling into KV cache compression design, our method excels in memory-constrained settings, preserves long-context understanding ability, and significantly reduces memory usage with minimal performance trade-offs compared to the baselines.

REFERENCES

- 540
541
542 Josh Achiam, Steven Adler, Sandhini Agarwal, Lama Ahmad, Ilge Akkaya, Florencia Leoni Aleman,
543 Diogo Almeida, Janko Altenschmidt, Sam Altman, Shyamal Anadkat, et al. Gpt-4 technical report.
544 *arXiv preprint arXiv:2303.08774*, 2023.
- 545 Yushi Bai, Xin Lv, Jiajie Zhang, Hongchang Lyu, Jiankai Tang, Zhidian Huang, Zhengxiao Du, Xiao
546 Liu, Aohan Zeng, Lei Hou, et al. Longbench: A bilingual, multitask benchmark for long context
547 understanding. *arXiv preprint arXiv:2308.14508*, 2023.
- 548 Liang Chen, Haozhe Zhao, Tianyu Liu, Shuai Bai, Junyang Lin, Chang Zhou, and Baobao Chang.
549 An image is worth 1/2 tokens after layer 2: Plug-and-play inference acceleration for large vision-
550 language models. *arXiv preprint arXiv:2403.06764*, 2024a.
- 551 Yukang Chen, Shengju Qian, Haotian Tang, Xin Lai, Zhijian Liu, Song Han, and Jiaya Jia. Longlora:
552 Efficient fine-tuning of long-context large language models. *arXiv preprint arXiv:2309.12307*,
553 2023.
- 554
555 Zhuoming Chen, Ranajoy Sadhukhan, Zihao Ye, Yang Zhou, Jianyu Zhang, Niklas Nolte, Yuandong
556 Tian, Matthijs Douze, Leon Bottou, Zhihao Jia, and Beidi Chen. Magicpig: Lsh sampling for
557 efficient llm generation, 2024b. URL <https://arxiv.org/abs/2410.16179>.
- 558 Wei-Lin Chiang, Zhuohan Li, Zi Lin, Ying Sheng, Zhanghao Wu, Hao Zhang, Lianmin Zheng,
559 Siyuan Zhuang, Yonghao Zhuang, Joseph E. Gonzalez, Ion Stoica, and Eric P. Xing. Vicuna: An
560 open-source chatbot impressing gpt-4 with 90%* chatgpt quality, March 2023. URL <https://lmsys.org/blog/2023-03-30-vicuna/>.
- 561
562 Pradeep Dasigi, Kyle Lo, Iz Beltagy, Arman Cohan, Noah A Smith, and Matt Gardner. A dataset of
563 information-seeking questions and answers anchored in research papers. In *Proceedings of the*
564 *2021 Conference of the North American Chapter of the Association for Computational Linguistics:*
565 *Human Language Technologies*, pages 4599–4610, 2021.
- 566
567 Yiran Ding, Li Lyna Zhang, Chengruidong Zhang, Yuanyuan Xu, Ning Shang, Jiahang Xu, Fan Yang,
568 and Mao Yang. Longrope: Extending llm context window beyond 2 million tokens. *arXiv preprint*
569 *arXiv:2402.13753*, 2024.
- 570
571 Harry Dong, Xinyu Yang, Zhenyu Zhang, Zhangyang Wang, Yuejie Chi, and Beidi Chen. Get more
572 with less: Synthesizing recurrence with kv cache compression for efficient llm inference. *arXiv*
573 *preprint arXiv:2402.09398*, 2024.
- 574 Alexander Fabbri, Irene Li, Tianwei She, Suyi Li, and Dragomir Radev. Multi-news: A large-
575 scale multi-document summarization dataset and abstractive hierarchical model. In Anna
576 Korhonen, David Traum, and Lluís Màrquez, editors, *Proceedings of the 57th Annual Meet-*
577 *ing of the Association for Computational Linguistics*, pages 1074–1084, Florence, Italy, July
578 2019a. Association for Computational Linguistics. doi: 10.18653/v1/P19-1102. URL <https://aclanthology.org/P19-1102>.
- 579
580 Alexander Richard Fabbri, Irene Li, Tianwei She, Suyi Li, and Dragomir Radev. Multi-news: A large-
581 scale multi-document summarization dataset and abstractive hierarchical model. In *Proceedings*
582 *of the 57th Annual Meeting of the Association for Computational Linguistics*, pages 1074–1084,
583 2019b.
- 584 Yao Fu, Rameswar Panda, Xinyao Niu, Xiang Yue, Hannaneh Hajishirzi, Yoon Kim, and Hao Peng.
585 Data engineering for scaling language models to 128k context. *arXiv preprint arXiv:2402.10171*,
586 2024.
- 587
588 Suyu Ge, Yunan Zhang, Liyuan Liu, Minjia Zhang, Jiawei Han, and Jianfeng Gao. Model tells you
589 what to discard: Adaptive kv cache compression for llms. *arXiv preprint arXiv:2310.01801*, 2023.
- 590
591 Bogdan Gliwa, Iwona Mochol, Maciej Biesek, and Aleksander Wawer. Samsun corpus: A human-
592 annotated dialogue dataset for abstractive summarization. *EMNLP-IJCNLP 2019*, page 70, 2019.
- 593
594 Daya Guo, Canwen Xu, Nan Duan, Jian Yin, and Julian McAuley. Longcoder: A long-range
595 pre-trained language model for code completion. *arXiv preprint arXiv:2306.14893*, 2023.

- 594 Chi Han, Qifan Wang, Wenhan Xiong, Yu Chen, Heng Ji, and Sinong Wang. Lm-infinite: Simple
595 on-the-fly length generalization for large language models. *arXiv preprint arXiv:2308.16137*,
596 2023.
- 597 Xanh Ho, Anh-Khoa Duong Nguyen, Saku Sugawara, and Akiko Aizawa. Constructing a multi-hop
598 qa dataset for comprehensive evaluation of reasoning steps. In *Proceedings of the 28th International*
599 *Conference on Computational Linguistics*, pages 6609–6625, 2020.
- 601 Luyang Huang, Shuyang Cao, Nikolaus Parulian, Heng Ji, and Lu Wang. Efficient attentions for
602 long document summarization. In *Proceedings of the 2021 Conference of the North American*
603 *Chapter of the Association for Computational Linguistics: Human Language Technologies*, pages
604 1419–1436, 2021.
- 605 Albert Q Jiang, Alexandre Sablayrolles, Arthur Mensch, Chris Bamford, Devendra Singh Chaplot,
606 Diego de las Casas, Florian Bressand, Gianna Lengyel, Guillaume Lample, Lucile Saulnier, et al.
607 Mistral 7b. *arXiv preprint arXiv:2310.06825*, 2023.
- 608 Huiqiang Jiang, Yucheng Li, Chengruidong Zhang, Qianhui Wu, Xufang Luo, Surin Ahn, Zhenhua
609 Han, Amir H Abdi, Dongsheng Li, Chin-Yew Lin, et al. Minference 1.0: Accelerating pre-filling
610 for long-context llms via dynamic sparse attention. *arXiv preprint arXiv:2407.02490*, 2024.
- 611 Mandar Joshi, Eunsol Choi, Daniel S Weld, and Luke Zettlemoyer. Triviaqa: A large scale distantly
612 supervised challenge dataset for reading comprehension. In *Proceedings of the 55th Annual*
613 *Meeting of the Association for Computational Linguistics (Volume 1: Long Papers)*, pages 1601–
614 1611, 2017.
- 615 Tomáš Kočiský, Jonathan Schwarz, Phil Blunsom, Chris Dyer, Karl Moritz Hermann, Gábor Melis,
616 and Edward Grefenstette. The narrativeqa reading comprehension challenge. *Transactions of the*
617 *Association for Computational Linguistics*, 6:317–328, 2018.
- 618 Wonbeom Lee, Jungi Lee, Junghwan Seo, and Jaewoong Sim. Infinigen: Efficient generative
619 inference of large language models with dynamic kv cache management, 2024. URL <https://arxiv.org/abs/2406.19707>.
- 620 Xin Li and Dan Roth. Learning question classifiers. In *COLING 2002: The 19th International*
621 *Conference on Computational Linguistics*, 2002.
- 622 Yuhong Li, Yingbing Huang, Bowen Yang, Bharat Venkitesh, Acyr Locatelli, Hanchen Ye, Tianle Cai,
623 Patrick Lewis, and Deming Chen. Snapkv: Llm knows what you are looking for before generation.
624 *arXiv preprint arXiv:2404.14469*, 2024.
- 625 Nelson F. Liu, Kevin Lin, John Hewitt, Ashwin Paranjape, Michele Bevilacqua, Fabio Petroni, and
626 Percy Liang. Lost in the middle: How language models use long contexts, 2023a.
- 627 Tianyang Liu, Canwen Xu, and Julian McAuley. Repobench: Benchmarking repository-level code
628 auto-completion systems, 2023b.
- 629 Baptiste Roziere, Jonas Gehring, Fabian Gloeckle, Sten Sootla, Itai Gat, Xiaoqing Ellen Tan, Yossi
630 Adi, Jingyu Liu, Tal Remez, Jérémy Rapin, et al. Code llama: Open foundation models for code.
631 *arXiv preprint arXiv:2308.12950*, 2023.
- 632 Mingjie Sun, Xinlei Chen, J Zico Kolter, and Zhuang Liu. Massive activations in large language
633 models. *arXiv preprint arXiv:2402.17762*, 2024.
- 634 Hugo Touvron, Thibaut Lavril, Gautier Izacard, Xavier Martinet, Marie-Anne Lachaux, Timothée
635 Lacroix, Baptiste Rozière, Naman Goyal, Eric Hambro, Faisal Azhar, et al. Llama: Open and
636 efficient foundation language models. *arXiv preprint arXiv:2302.13971*, 2023a.
- 637 Hugo Touvron, Louis Martin, Kevin Stone, Peter Albert, Amjad Almahairi, Yasmine Babaei, Nikolay
638 Bashlykov, Soumya Batra, Prajjwal Bhargava, Shruti Bhosale, et al. Llama 2: Open foundation
639 and fine-tuned chat models. *arXiv preprint arXiv:2307.09288*, 2023b.

- 648 Daniel Waddington, Juan Colmenares, Jilong Kuang, and Fengguang Song. Kv-cache: A scal-
649 able high-performance web-object cache for manycore. In *2013 IEEE/ACM 6th International*
650 *Conference on Utility and Cloud Computing*, pages 123–130. IEEE, 2013.
- 651 Lean Wang, Lei Li, Damai Dai, Deli Chen, Hao Zhou, Fandong Meng, Jie Zhou, and Xu Sun. Label
652 words are anchors: An information flow perspective for understanding in-context learning. *arXiv*
653 *preprint arXiv:2305.14160*, 2023.
- 654 Wenhao Wu, Yizhong Wang, Guangxuan Xiao, Hao Peng, and Yao Fu. Retrieval head mechanistically
655 explains long-context factuality. *arXiv preprint arXiv:2404.15574*, 2024.
- 656 Guangxuan Xiao, Yuandong Tian, Beidi Chen, Song Han, and Mike Lewis. Efficient streaming
657 language models with attention sinks. *arXiv preprint arXiv:2309.17453*, 2023.
- 658 Dongjie Yang, XiaoDong Han, Yan Gao, Yao Hu, Shilin Zhang, and Hai Zhao. Pyramidinfer: Pyramid
659 kv cache compression for high-throughput llm inference. *arXiv preprint arXiv:2405.12532*, 2024.
- 660 Zhilin Yang, Peng Qi, Saizheng Zhang, Yoshua Bengio, William Cohen, Ruslan Salakhutdinov,
661 and Christopher D Manning. Hotpotqa: A dataset for diverse, explainable multi-hop question
662 answering. In *Proceedings of the 2018 Conference on Empirical Methods in Natural Language*
663 *Processing*, pages 2369–2380, 2018.
- 664 Zhenyu Zhang, Ying Sheng, Tianyi Zhou, Tianlong Chen, Lianmin Zheng, Ruisi Cai, Zhao Song,
665 Yuandong Tian, Christopher Ré, Clark Barrett, et al. H2o: Heavy-hitter oracle for efficient
666 generative inference of large language models. *Advances in Neural Information Processing*
667 *Systems*, 36, 2024.
- 668 Ming Zhong, Da Yin, Tao Yu, Ahmad Zaidi, Mutethia Mutuma, Rahul Jha, Ahmed Hassan, Asli
669 Celikyilmaz, Yang Liu, Xipeng Qiu, et al. Qmsum: A new benchmark for query-based multi-
670 domain meeting summarization. In *Proceedings of the 2021 Conference of the North American*
671 *Chapter of the Association for Computational Linguistics: Human Language Technologies*, pages
672 5905–5921, 2021.
- 673 Dawei Zhu, Nan Yang, Liang Wang, Yifan Song, Wenhao Wu, Furu Wei, and Sujian Li. Pose:
674 Efficient context window extension of llms via positional skip-wise training. *arXiv preprint*
675 *arXiv:2309.10400*, 2023.
- 676
677
678
679
680
681
682
683
684
685
686
687
688
689
690
691
692
693
694
695
696
697
698
699
700
701

A LIMITATIONS

Our experiments were limited to three base models: LLAMA-3-8B-Instruct, LLAMA-3-70B-Instruct and Mistral-7B-Instruct. While these models demonstrated consistent trends, the robustness of our findings could be enhanced by testing a broader array of model families, should resources permit. Additionally, our research was conducted exclusively in English, with no investigations into how these findings might be transferred to other languages. Expanding the linguistic scope of our experiments could provide a more comprehensive understanding of the applicability of our results globally. Based on our results at LongBench and Needle-in-a-HayStack experiment, PyramidKV generally works decently in most of the language tasks (i.e., Single-Document QA, Multi-Document QA, Summarization, Few-Shot In-Context Learning, etc.). Although we observe that PyramidKV performs better in some tasks (i.e., Few-Shot In-Context Learning) compared with some other tasks (i.e., Summarization), we have not observed cases that the decoding result collapses at some tasks. This remains a new topic for future work to explore.

B FUTURE WORK

Our investigation on PyramidKV highlights considerable opportunities for optimizing KV cache compression by adjusting the number of KV caches retained according to the distinct attention patterns of each layer (or even for each head). For instance, the retention of KV cache for each layer could be dynamically modified based on real-time analysis of the attention matrices, ensuring that the compression strategy is consistently aligned with the changing attention dynamics within LLMs. Furthermore, our experiments indicate that PyramidKV significantly surpasses other methods in few-shot learning tasks, suggesting promising applications of KV cache in in-context learning. This approach could potentially enable the use of more shots within constrained memory limits.

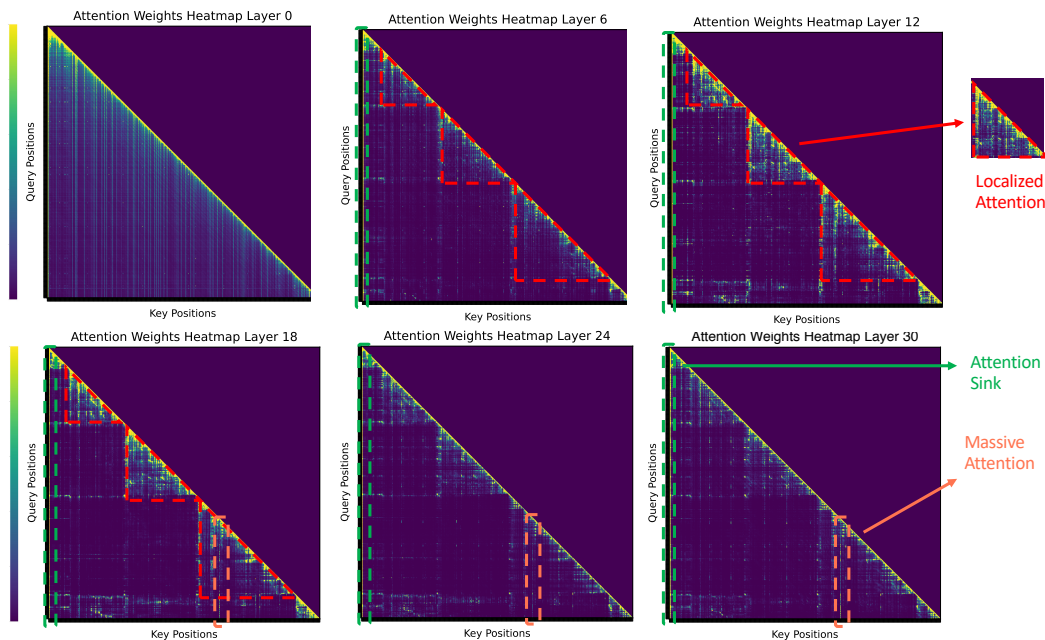


Figure 5: Attention patterns of retrieval-augmented generation across layers in Mistral-7B-Instruct model (Jiang et al., 2023)

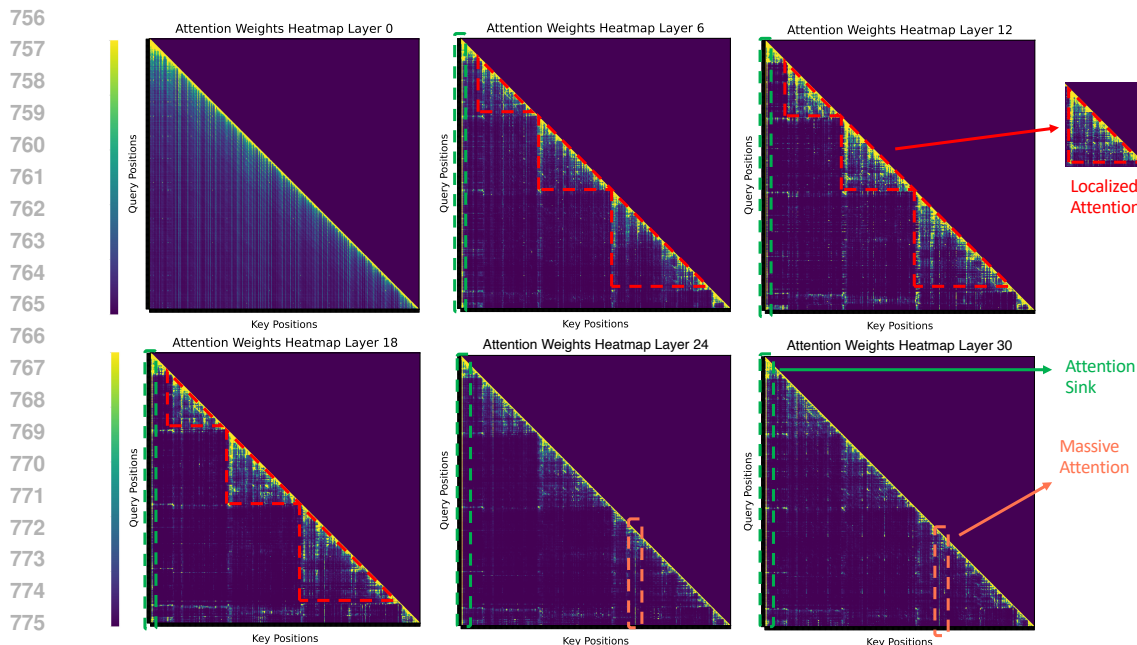


Figure 6: Attention patterns of retrieval-augmented generation across layers in Mistral-8x7B-Instruct Mixture-of-Experts model.

C PYRAMIDAL INFORMATION FUNNELING

Figure 5 and Figure 6 shows the attention patterns of one QA example over six different layers (i.e., 0, 6, 12, 18, 24, and 30) for Mistral-7B-Instruct model and Mistral-8x7B-Instruct Mixture-of-Experts model. Figure 5 and Figure 6 demonstrate that the Pyramidal Information Funneling phenomenon is also evident in both the Mistral model and Mistral model. The results reveal that, akin to Llama-like models, Mistral exhibit a progressively narrowing attention focus across layers. This supports the universality of the Pyramidal Information Funneling phenomenon across diverse model families. We hope this addresses your concern and underscores the generalizability of our findings.

Our analysis uniquely examines attention metrics across all transformer layers, from 0 to 30, leading to the discovery of a key phenomenon we term Pyramidal Information Funneling.

Lee et al. (2024) conducted a limited investigation into attention patterns, focusing only on the lower layer (layer 0) and a single upper layer (layer 18). While Lee et al. (2024) noted that attention becomes more skewed in upper layers, it did not provide a fine-grained observation of attention patterns across all layers. In contrast, our study reveals several novel findings:

- **Localized Attention:** We observe that attention progressively narrows its focus, targeting specific components within the input sequence.
- **Massive Attention Mechanism:** In the upper layers, attention heavily concentrates on a small set of critical tokens. Notably, these tokens are not limited to the leading positions, as observed in Lee et al. (2024), but also appear at regular intervals across the sequence. The discrepancy arises from differences in input settings, with Lee et al. (2024) identifying massive attention only at the initial tokens.

These insights motivated us to propose a token-selection method based on the highest attention scores in the upper layers, rather than solely relying on tokens from earlier positions.

To the best of our knowledge, Chen et al. (2024b) has not analyzed attention patterns across transformer layers.

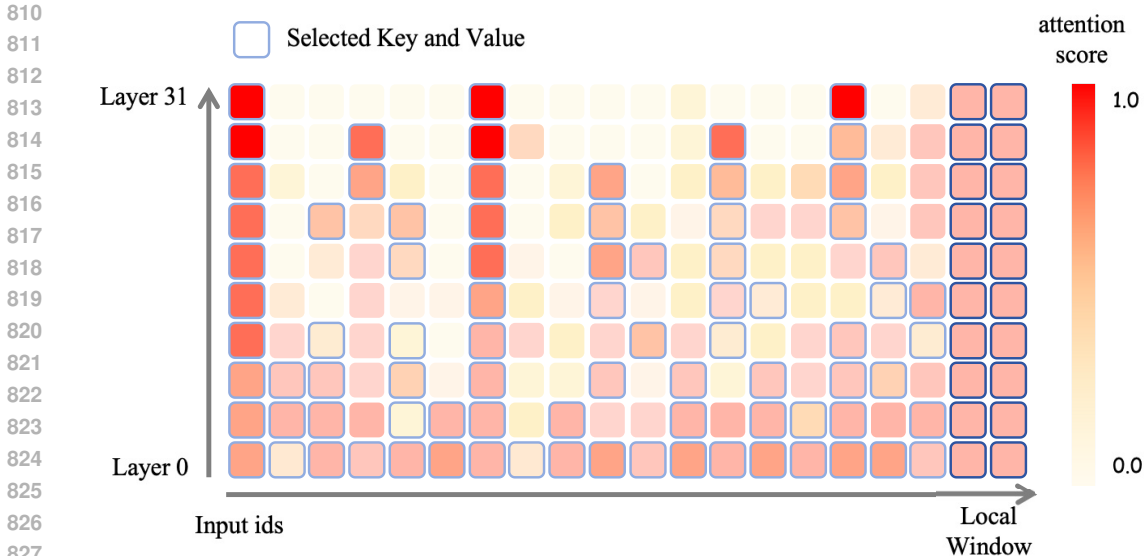


Figure 7: Illustration of PyramidKV. At the lower level of the transformer, the PyramidKV selects more keys and values based on the exhibited average attention pattern. Fewer keys and values at the higher level are selected based on the massive activation pattern, where we observe that attention scores are concentrated over local regions.

Therefore, although Lee et al. (2024) and Chen et al. (2024b) are considered contemporaneous with our work, making a comparison unnecessary, the perspective of our observation is considered novel compared with Lee et al. (2024) and Chen et al. (2024b). Moreover, although Lee et al. (2024) also observed attention patterns, the method we proposed based on our observations is significantly different from Lee et al. (2024), further highlighting the novelty of our work.

D DETAILS OF PROPOSED METHOD

Based on the pyramidal information funneling observed across different layers, PyramidKV consists of two steps: (1) Dynamically allocating different KV cache sizes/budgets across different layers; and (2) Selecting important KV vectors in each attention head for caching as Figure 7.

Our decision to use an arithmetic sequence is driven by three key factors:

- **Alignment with Pyramidal Information Funneling Pattern:** Empirical observations reveal a pyramidal information funneling pattern, where lower layers exhibit dispersed attention while higher layers concentrate on fewer tokens. Inspired by this, we adopt the arithmetic sequence design to align with this natural progression.
- **Superior Empirical Performance:** Through extensive experimentation across diverse datasets, we compared various methods, including the arithmetic sequence and adaptive approaches. Results consistently showed that the arithmetic sequence method outperformed others.
- **Computational Efficiency:** The arithmetic sequence method introduces minimal computational overhead compared to adaptive approaches, which require dynamically computing cache budgets across layers.

To perform KV cache eviction, we use torch.gather. Below, we outline the memory allocation and release process of torch.gather:

- **Index Selection:** Identify the positions of the elements to extract from the input tensor.

- **Memory Location Calculation:** Compute the specific memory locations of the elements to be extracted using the strides of the input tensor across each dimension.
- **Output Tensor Creation:** Allocate memory to create a new output tensor and copy the selected elements to their corresponding positions in the output tensor.
- **Memory Management:** Since torch.gather is not an in-place operation, it creates a new tensor to store the results, while the memory of the original input tensor is released.

The speed-up offered by PyramidKV is complementary to that achieved through tensor parallelism and pipeline parallelism, as these approaches are not mutually exclusive. PyramidKV can be seamlessly integrated with both tensor parallelism and pipeline parallelism.

E DETAILS OF EVALUATION

We use LongBench (Bai et al., 2023) to assess the performance of PyramidKV on tasks involving long-context inputs. LongBench is a meticulously designed benchmark suite that tests the capabilities of language models in handling extended documents and complex information sequences. This benchmark was created for multi-task evaluation of long context inputs.

We present the details of metrics, language and data for LongBench at Table 3.

We run all the experiments on NVIDIA A100.

Dataset	Source	Avg len	Metric	Language	#data
<i>Single-Document QA</i>					
NarrativeQA	Literature, Film	18,409	F1	English	200
Qasper	Science	3,619	F1	English	200
MultiFieldQA-en	Multi-field	4,559	F1	English	150
<i>Multi-Document QA</i>					
HotpotQA	Wikipedia	9,151	F1	English	200
2WikiMultihopQA	Wikipedia	4,887	F1	English	200
MuSiQue	Wikipedia	11,214	F1	English	200
<i>Summarization</i>					
GovReport	Government report	8,734	Rouge-L	English	200
QMSum	Meeting	10,614	Rouge-L	English	200
MultiNews	News	2,113	Rouge-L	English	200
<i>Few-shot Learning</i>					
TREC	Web question	5,177	Accuracy (CLS)	English	200
TriviaQA	Wikipedia, Web	8,209	F1	English	200
SAMSum	Dialogue	6,258	Rouge-L	English	200
<i>Synthetic Task</i>					
PassageCount	Wikipedia	11,141	Accuracy (EM)	English	200
PassageRetrieval-en	Wikipedia	9,289	Accuracy (EM)	English	200
<i>Code Completion</i>					
LCC	Github	1,235	Edit Sim	Python/C#/Java	500
RepoBench-P	Github repository	4,206	Edit Sim	Python/Java	500

Table 3: An overview of the dataset statistics in LongBench (Bai et al., 2023). ‘Source’ denotes the origin of the context. ‘Accuracy (CLS)’ refers to classification accuracy, while ‘Accuracy (EM)’ refers to exact match accuracy.

F LICENSE

LongBench: MIT

G HANDLE ROTARY EMBEDDING AFTER TOKENS ARE REMOVED IN PYRAMIDKV

We keep the rotary embedding unchanged after tokens are removed, so that LLMs can still capture the exact position information even if the tokens are removed. StreamingLLM (Xiao et al., 2023) shows that rolling kv cache with the correct relative position is crucial for maintaining performance. This is because StreamingLLM is designed to mainly handle unlimited context sizes, where contexts exceed the LLM’s fixed context length. Without changing the rotary embedding after token removal, LLMs would receive rotary embedding of a non-monotonic position sequence. For example, after the first KV cache compression, LLMs might receive the input position embedding as $[0, 1, 2, 3, 3096, 3097, \dots, 4096]$, and the position embedding of the generated sequences could be $[1005, 1006, 1007, \dots]$. The position sequence of $[0, 1, 2, 3, 3096, \dots, 4096, 1005, 1006, 1007, \dots]$ is a non-monotonic sequence, which may negatively hurt the performance. In contrast, our targeting settings will not process unlimited context size. For example, given an input sequence of 4012 length, after KV cache compression, the position sequence would be $[0, 4, 6, 16, \dots, 3927, 3987, 4012]$, and the position sequence of the generated tokens would be $[4013, 4014, \dots]$. By keeping the rotary embedding unchanged after the tokens are removed, the LLM avoids non-monotonic position sequences, and the LLM can capture the exact position information even if the tokens are shifted. Our preliminary results show that rolling KV cache with the correct relative position will slightly decrease the performance.

H ABLATION STUDY

In this section, we present an ablation study for hyperparameters and allocation strategies.

Based on our observations of the attention pattern, we find that a relatively stable, linear arithmetic decrease aligns more closely with the underlying structure of the pattern. We conduct experiments comparing various allocation strategies.

We conducted hyperparameter testing on the original development sets of 16 datasets in LongBench. The parameter β demonstrated remarkable stability, showing minimal sensitivity to varying hyperparameter settings, which highlights its robustness. Conversely, α consistently produced superior results when set to 8 or 16. Consequently, these values were adopted for subsequent experiments. In Appendix H.2 and H.3, we further analyzed the impact of hyperparameter selection on KV cache budget allocation across different layers. The experiments reaffirmed that β had negligible influence on the outcomes, underscoring its stability. Meanwhile, α continued to deliver optimal results at values of 8 and 16.

H.1 ALLOCATION STRATEGIES

Based on our observations of the attention pattern, we find that a relatively stable, linear arithmetic decrease aligns more closely with the underlying structure of the pattern.

We conduct experiments comparing various pyramidal allocation strategies (i.e., linear decay strategy, geometric decay strategy and exponential decay strategy) with a cache size of 64 as Table 4 to confirm that a linear strategy is indeed optimal or preferable.

We also propose three adaptive allocation baselines, which are based on the entropy, Gini coefficient, and sparsity of the attention values at each layer. The weight of each layer is calculated based on its corresponding metric (entropy, Gini coefficient, or sparsity), and the budget is allocated accordingly. Specifically:

- **Entropy-based allocation:** Layers with higher entropy receive higher weights. Each layer’s entropy is calculated based on the the layer’s attention.
- **Gini coefficient-based allocation:** Layers with higher Gini coefficients receive higher weights. Each layer’s Gini coefficient is calculated based on the the layer’s attention

The empirical results as Table 4 consistently showed that the linear strategy outperformed its counterparts, establishing it as the most effective approach for our use case. The experiment strengthens the rationale for choosing the specific allocation method.

Stra.	Single-Document QA			Multi-Document QA			Summarization			Few-shot Learning			Synthetic		Code		Avg.
	NrrvQA	Qasper	MF-en	HotpotQA	2WikiMQA	Musique	GovReport	QMSum	MultiNews	TREC	TriviaQA	SAMSum	PCount	Pre	Lcc	RB-P	
Geo.	20.51	15.04	29.4	34.93	26.41	16.6	18.32	21.68	18.81	52	87.51	36.15	5.18	69.17	53.11	44.91	34.36
Exp.	20.58	14.82	28.74	34.34	26.24	16.11	18.41	21.63	18.75	52.00	87.94	36.26	5.19	69.17	54.34	43.21	34.23
Lin.	21.13	14.18	30.26	35.12	23.76	16.17	18.33	21.65	19.23	58.00	88.31	37.07	5.23	69.50	52.61	45.74	34.76
Entropy.	18.12	14.12	27.22	33.21	21.16	15.16	17.76	19.87	17.09	51	87.31	34.29	5.09	68.91	50.12	42.98	32.71
Gini.	17.92	14.61	28.21	32.67	19.98	15.98	16.20	19.29	18.21	51.00	86.21	34.97	5.11	65.51	51.98	43.37	32.58

Table 4: Ablation study of allocation strategies.

H.2 HYPER PARAMETER α

We present the study of α for LLaMa-3-8B-Instruct in 128 KV cache size budget at Table 5. We find that a small alpha value (i.e., 8, 16) leads to better performance than a larger alpha value (i.e., 24, 32, 40, 48).

α	Single-Document QA			Multi-Document QA			Summarization			Few-shot Learning			Synthetic		Code		Avg.
	NrrvQA	Qasper	MF-en	HotpotQA	2WikiMQA	Musique	GovReport	QMSum	MultiNews	TREC	TriviaQA	SAMSum	PCount	Pre	Lcc	RB-P	
8	21.40	16.92	31.62	38.45	28.72	18.59	19.96	22.49	20.96	66.50	89.35	38.43	5.92	69.00	57.86	51.80	37.37
16	23.37	16.21	33.93	38.24	27.28	20.57	19.71	21.93	20.86	60.00	88.75	38.34	5.48	69.12	57.84	53.42	37.19
24	22.85	14.51	32.26	38.38	28.36	20.33	19.55	21.72	20.72	54.50	88.71	38.46	5.48	69.50	56.83	53.65	36.61
32	23.01	14.54	31.68	38.86	29.90	19.16	19.20	21.83	20.52	49.50	87.01	38.01	5.75	69.50	57.02	54.54	36.25
40	21.70	13.06	30.14	36.78	27.34	18.88	18.72	21.37	19.79	44.00	87.74	38.43	6.08	69.25	56.11	53.89	35.21
48	21.51	12.30	29.77	39.04	26.76	17.97	18.65	21.20	20.29	44.50	87.73	38.44	5.51	69.25	56.73	53.88	35.22

Table 5: Ablation on α .

H.3 HYPER PARAMETER β

One topic we want to analyze for our ablation study is the selection of β , which can determine the staircase. The smaller β is, the gentler the staircase is; the larger β is, the steeper the staircase is. We want to investigate the effect of β step size on the final result. Results on 128 KV cache size and LLaMa-3-8B-Instruct are shown in Table 6. The results at Table 6 show that using a relatively small value of β yields better outcomes, and PyramidKV is generally robust to the selection of β .

β	Single-Document QA			Multi-Document QA			Summarization			Few-shot Learning			Synthetic		Code		Avg.
	NrrvQA	Qasper	MF-en	HotpotQA	2WikiMQA	Musique	GovReport	QMSum	MultiNews	TREC	TriviaQA	SAMSum	PCount	Pre	Lcc	RB-P	
20	21.40	16.92	33.79	39.73	28.72	18.59	19.86	22.48	20.95	66.50	89.35	38.39	5.92	69.00	56.49	47.95	37.25
18	21.71	16.24	33.59	39.89	27.94	18.38	19.76	22.32	21.20	66.50	88.98	38.93	5.46	69.50	56.47	49.23	37.25
16	21.74	14.86	33.64	39.18	28.17	18.77	19.57	22.25	21.48	66.50	89.69	38.87	5.82	69.50	57.02	50.11	37.32
14	22.53	16.31	33.50	40.50	28.15	19.26	19.66	22.39	21.38	65.50	90.02	38.56	5.75	69.50	57.51	49.71	37.51

Table 6: Ablation on β .

I INTEGRATION WITH MINFERENCE

We would like to clarify that PyramidKV and MInference Jiang et al. (2024) are complementary approaches addressing different aspects of KV cache optimization. Specifically:

- MInference focuses on accelerating the generation of KV caches during the pre-filling stage of LLM inference.

- In contrast, PyramidKV targets efficient KV cache management during LLM decoding.

To evaluate their respective strengths, we compared PyramidKV and MInference on Longbench using a KV cache size of 128. The results demonstrated the superior performance of PyramidKV.

Furthermore, we demonstrate that MInference and PyramidKV can be seamlessly integrated to achieve highly efficient inference while maintaining performance comparable to full attention. The results of MInference combined with PyramidKV, evaluated on Longbench with a KV cache size of 128, as PyramidKV + MInference hybrid approach.

Stra.	Single-Document QA			Multi-Document QA			Summarization			Few-shot Learning			Synthetic		Code		Avg.
	NrrvQA	Qasper	MF-en	HotpotQA	2WikiMQA	Musique	GovReport	QMSum	MultiNews	TREC	TriviaQA	SAMSum	PCount	Pre	Lcc	RB-P	
PyramidKV	23.99	20.61	38.28	43.23	31.62	20.94	21.27	22.69	22.83	71	90.48	39.86	5.83	69.25	56.94	50.16	39.31
MInference	19.74	30.63	40.41	44.28	35.22	20.65	28.43	23.35	26.75	72.00	87.90	42.78	6.30	64.00	58.76	5.06	38.86
M. + P.	20.04	31.74	39.98	43.10	35.21	21.60	27.41	23.06	26.76	73.00	88.03	43.36	6.28	64.00	58.57	45.42	40.47

Table 7: Comparison between PyramidKV, MInference and MInference-PyramidKV hybrid method.

In summary, we demonstrate that PyramidKV outperforms MInference on Longbench. Furthermore, when integrated with MInference, PyramidKV enhances its performance even further.

J COMPARISON WITH PYRAMIDINFER

Our work differs from PyramidInfer in two key aspects:

- **Decay Strategy:** While PyramidInfer Yang et al. (2024) employs a geometric decay strategy, our method adopts an arithmetic decay strategy. We argue that the relatively stable and linear nature of arithmetic decay better aligns with the behavior of the attention mechanism. This strategy is derived from empirically observed attention patterns, aiming to closely match them. Notably, our approach also achieves superior results, as demonstrated in the experimental results presented in the table below.
- **Token Selection:** PyramidInfer discards tokens in earlier layers, preventing them from being reconsidered in later layers. In contrast, our method allows previously discarded tokens to be re-evaluated in higher layers, recognizing that these tokens may still hold relevance at different stages of the model’s processing.
- **Pyramidal Information Funneling Pattern:** A key contribution of our work lies in identifying and leveraging the pyramidal information funneling phenomenon within attention mechanisms. Through in-depth analysis, we observe that attention tends to disperse in earlier layers and progressively concentrates on crucial tokens in higher layers. This insight forms the foundation of our arithmetic decay strategy, ensuring that our method aligns more naturally with these intrinsic patterns.

Despite some similarities between the two approaches, these differences lead to significantly distinct outcomes. As shown in Table 8, our method consistently outperforms PyramidInfer, highlighting the effectiveness of our design choices.

Stra.	Single-Document QA			Multi-Document QA			Summarization			Few-shot Learning			Synthetic		Code		Avg.
	NrrvQA	Qasper	MF-en	HotpotQA	2WikiMQA	Musique	GovReport	QMSum	MultiNews	TREC	TriviaQA	SAMSum	PCount	Pre	Lcc	RB-P	
Pyramidinfer	20.42	12.77	25.21	35.81	25.83	16.88	18.27	21.78	18.52	51.00	88.54	35.76	5.61	69.25	53.21	44.12	33.94
PyramidKV	21.13	14.18	30.26	35.12	23.76	16.17	18.33	21.65	19.23	58.00	88.31	37.07	5.23	69.50	52.61	45.74	34.76

Table 8: Comparison between PyramidKV and Pyramidinfer.

K PYRAMIDKV WILL CAUSE MINIMAL EXTRA INFERENCE OVERHEAD.

The allocation strategy and score-based selection add minimal complexity in the inference phase compared to the computation required for next-token predictions as Table 9. Each row shows the

setting of using a specific “[Prompt length, Generation length]” combination. We show the inference speed comparison between total inference time, time for allocation strategy and time for score-based selection on LLaMa-3-8B-Instruct. Each cell is the latency measured in seconds. Furthermore, our budget allocation can be calculated before inference, requiring only a one-time computation. Thus, PyramidKV will cause minimal extra inference overhead.

Prompt Length	Generation Length	Inference Time	Allocation Time	Selection Time
512	512	18.26	0.000003	0.0194
512	1024	34.69	0.000002	0.0133
512	2048	70.69	0.000003	0.013
512	4096	138.62	0.000005	0.013
1024	512	17.32	0.000002	0.0131
1024	1024	34.67	0.000002	0.01288
1024	2048	70.21	0.000005	0.01296
1024	4096	138.61	0.000003	0.01297
2048	512	17.48	0.000004	0.0128
2048	1024	34.78	0.000006	0.0129
2048	2048	69.50	0.000003	0.01297
2048	4096	138.59	0.000003	0.013
4096	512	17.58	0.000002	0.013
4096	1024	34.93	0.000004	0.0129
4096	2048	69.65	0.000002	0.013
4096	4096	138.87	0.000002	0.013

Table 9: Extra inference overhead of PyramidKV

L INFERENCE SPEED COMPARISON

PyramidKV does not require extra computation time for budget allocation at inference by design. We show the inference speed comparison between PyramidKV and baselines on LLaMa-3-8B-Instruct as Table 10. Each row shows the setting of using a specific “[Prompt length, Generation length]” combination. Each cell is the latency measured in seconds. PyramidKV does not sacrifice the speed. PyramidKV provides performance improvement and memory saving while runs at a comparable speed compared with baselines (i.e. SnapKV (Li et al., 2024), StreamingLLM (Xiao et al., 2023) and H2O (Zhang et al., 2024)). That’s because the allocation strategy requires very limited additional complexity in the inference/generation phase compared with computation required for generation as Appendix K.

Prompt Length	Generation Length	H2O	SnapKV	StreamingLLM	PyramidKV
512	512	18.47	18.25	18.96	18.26
512	1024	35.10	34.76	36.20	34.69
512	2048	70.21	69.60	72.35	70.69
512	4096	140.80	139.42	146.37	138.62
1024	512	17.63	17.34	18.12	17.32
1024	1024	35.16	34.61	36.17	34.67
1024	2048	71.02	69.17	72.37	70.21
1024	4096	140.51	138.83	146.09	138.61
2048	512	17.64	19.54	18.22	17.48
2048	1024	35.09	34.76	36.29	34.78
2048	2048	70.84	69.56	72.46	69.50
2048	4096	140.16	139.55	145.22	138.59
4096	512	17.75	17.67	18.40	17.58
4096	1024	35.20	35.08	36.46	34.93
4096	2048	70.02	69.26	72.58	69.65
4096	4096	139.87	138.57	144.98	138.87

Table 10: Performance comparison across different configurations and methods.

1134 M PYRAMIDKV EXCELS IN ALL KV CACHE SIZE LIMITATION
1135

1136 The evaluation results from LongBench(Bai et al., 2023) are shown in Table 11, Table 12, and Table 13.
1137 We report the results using LLaMa-3-8B-Instruct, LLaMa-3-70B-Instruct and Mistral-7B-Instruct(Jiang
1138 et al., 2023) for different KV cache sizes.

1139 Overall, PyramidKV consistently surpasses other method across a range of KV cache sizes and
1140 different backbone models, with its performance advantages becoming particularly pronounced in
1141 memory-constrained environments. Upon examining specific tasks, PyramidKV demonstrates a
1142 notably superior performance on the TREC task, a few-shot question answering challenge. This
1143 suggests that the model effectively aggregates information from the few-shot examples, highlighting
1144 the potential for further investigation into in-context learning tasks.
1145

1146
1147
1148
1149
1150
1151
1152
1153
1154
1155
1156
1157
1158
1159
1160
1161
1162
1163
1164
1165
1166
1167
1168
1169
1170
1171
1172
1173
1174
1175
1176
1177
1178
1179
1180
1181
1182
1183
1184
1185
1186
1187

1188
1189
1190
1191
1192
1193
1194
1195
1196
1197
1198
1199
1200
1201
1202
1203
1204
1205
1206
1207
1208
1209

Method	Single-Document QA			Multi-Document QA			Summarization			Few-shot Learning			Synthetic		Code		
	NrrvQA	Qasper	MF-en	HotpotQA	2WikiMQA	Musique	GovReport	QMSum	MultiNews	TREC	TriviaQA	SAMSum	PCount	Pre	Lcc	RB-P	Avg.
	18409	3619	4559	9151	4887	11214	8734	10614	2113	5177	8209	6258	11141	9289	1235	4206	
LLaMa-3-8B-Instruct, KV Size = Full																	
FKV	25.70	29.75	41.12	45.55	35.87	22.35	25.63	23.03	26.21	73.00	90.56	41.88	04.67	69.25	58.05	50.77	41.46
LLaMa-3-8B-Instruct, KV Size = 64																	
SKV	19.86	9.09	27.89	37.34	28.35	18.17	15.86	20.80	16.41	38.50	85.92	36.32	5.22	69.00	51.78	48.38	33.05
H2O	20.80	11.34	27.03	37.25	30.01	17.94	18.29	21.49	19.13	38.00	84.70	37.76	5.63	69.33	53.44	50.15	33.89
SLM	17.44	8.68	22.25	35.37	31.51	15.97	15.46	20.06	14.64	38.00	72.33	29.10	5.42	69.50	46.14	45.09	30.43
Ours	21.13	14.18	30.26	35.12	23.76	16.17	18.33	21.65	19.23	58.00	88.31	37.07	5.23	69.50	52.61	45.74	34.76
LLaMa-3-8B-Instruct, KV Size = 96																	
SKV	20.45	10.34	31.84	37.85	28.65	18.52	17.90	21.26	19.07	41.50	86.95	37.82	5.08	69.12	54.69	51.31	34.51
H2O	21.55	11.21	28.73	37.66	30.12	18.47	19.57	21.57	20.44	38.50	87.63	38.47	5.60	69.00	54.51	50.16	34.57
SLM	18.67	8.43	24.98	38.35	30.59	16.37	17.33	19.84	18.41	41.00	73.92	29.38	5.80	69.50	47.15	45.61	31.58
Ours	21.67	15.10	33.50	39.73	26.48	17.47	19.64	22.28	20.49	61.50	87.38	38.18	6.00	69.25	55.30	46.78	36.29
LLaMa-3-8B-Instruct, KV Size = 128																	
SKV	21.19	13.55	32.64	38.75	29.64	18.73	18.98	21.62	20.26	45.00	88.36	37.64	5.13	68.85	55.84	51.82	35.50
H2O	22.12	13.20	31.61	37.79	32.71	18.45	20.32	22.02	21.10	38.50	87.75	39.14	5.83	69.50	55.06	50.97	35.37
SLM	18.61	9.65	25.99	37.95	29.39	16.34	18.03	20.11	20.08	43.50	74.08	29.86	5.90	69.50	47.47	45.60	32.00
Ours	21.40	16.92	33.79	39.73	28.72	18.59	19.86	22.48	20.95	66.50	89.35	38.39	5.92	69.00	56.49	47.95	37.25
LLaMa-3-8B-Instruct, KV Size = 2048																	
SKV	25.86	29.55	41.10	44.99	35.80	21.81	25.98	23.40	26.46	73.50	90.56	41.66	5.17	69.25	56.65	49.94	41.35
SLM	21.71	25.78	38.13	40.12	32.01	16.86	23.14	22.64	26.48	70.00	83.22	31.75	5.74	68.50	53.50	45.58	37.82
H2O	25.56	26.85	39.54	44.30	32.92	21.09	24.68	23.01	26.16	53.00	90.56	41.84	4.91	69.25	56.40	49.68	39.35
Ours	25.40	29.71	40.25	44.76	35.32	21.98	26.83	23.30	26.19	73.00	90.56	42.14	5.22	69.25	58.76	51.18	41.49

Table 11: Performance comparison of PyramidKV (Ours) with SnapKV (SKV), H2O, StreamingLLM (SLM) and FullKV (FKV) on LongBench for LLaMa-3-8B-Instruct. PyramidKV generally outperforms other KV Cache compression methods across various KV Cache sizes and LLMs. The performance strengths of PyramidKV are more evident in small KV Cache sizes. Bold text represents the best performance.

1209
1210
1211
1212
1213
1214
1215
1216
1217
1218
1219
1220
1221
1222
1223
1224
1225
1226
1227
1228
1229
1230
1231
1232
1233
1234
1235
1236
1237
1238
1239
1240
1241

Method	Single-Document QA			Multi-Document QA			Summarization			Few-shot Learning			Synthetic		Code		
	NrrvQA	Qasper	MF-en	HotpotQA	2WikiMQA	Musique	GovReport	QMSum	MultiNews	TREC	TriviaQA	SAMSum	PCount	Pre	Lcc	RB-P	Avg.
	18409	3619	4559	9151	4887	11214	8734	10614	2113	5177	8209	6258	11141	9289	1235	4206	
Mistral-7B-Instruct, KV Size = Full																	
FKV	26.90	33.07	49.20	43.02	27.33	18.78	32.91	24.21	26.99	71.00	86.23	42.65	2.75	86.98	56.96	54.52	42.71
Mistral-7B-Instruct, KV Size = 64																	
SKV	16.94	17.17	39.51	36.87	22.26	15.18	14.75	20.35	21.45	37.50	84.16	37.28	4.50	61.13	42.40	38.44	30.72
SLM	15.01	13.84	28.74	30.97	24.50	13.42	13.25	19.46	19.17	35.50	76.91	29.61	4.67	27.33	38.71	35.29	25.60
H2O	18.19	19.04	37.40	30.18	22.22	13.77	16.60	21.52	21.98	37.00	81.02	38.62	5.00	66.03	43.54	40.46	30.88
Ours	20.91	20.21	39.94	33.57	22.87	15.70	17.31	21.23	21.41	54.00	81.98	36.96	3.58	60.83	44.52	37.99	32.19
Mistral-7B-Instruct, KV Size = 96																	
SKV	19.92	18.80	43.29	39.66	23.08	15.94	16.65	21.26	21.47	43.50	83.48	39.74	4.00	60.10	45.53	41.12	32.47
SLM	15.15	15.48	31.44	30.03	23.93	12.73	16.76	19.15	19.19	41.50	75.31	28.71	5.00	28.48	38.92	36.05	26.37
H2O	19.44	20.81	38.78	32.39	21.51	14.43	17.68	22.40	21.99	38.00	82.51	39.94	6.06	77.48	45.18	42.43	32.67
Ours	20.35	21.87	41.15	34.94	21.85	15.81	18.21	21.66	21.43	65.00	83.60	39.60	4.50	67.80	45.83	39.38	34.08
Mistral-7B-Instruct, KV Size = 128																	
SKV	19.16	21.46	43.52	38.60	23.35	16.09	17.66	21.84	21.47	47.50	84.15	40.24	5.00	69.31	46.98	42.97	34.96
SLM	16.57	14.68	32.40	30.19	22.64	12.34	18.08	18.96	19.19	43.50	74.22	29.02	4.50	29.48	39.23	36.16	27.57
H2O	21.20	21.90	41.55	33.56	21.28	12.93	18.59	22.61	21.99	39.00	82.37	40.44	6.00	83.19	46.41	42.66	34.73
Ours	21.75	22.03	44.32	34.06	22.79	15.77	18.58	21.89	21.43	66.00	83.46	39.75	4.50	66.90	46.96	41.28	35.72
Mistral-7B-Instruct, KV Size = 2048																	
SKV	25.89	32.93	48.56	42.96	27.42	19.02	26.56	24.47	26.69	70.00	86.27	42.57	5.50	88.90	50.42	46.72	41.56
SLM	20.31	26.64	45.72	35.25	24.31	12.20	27.47	21.57	24.51	68.50	71.95	31.19	5.00	22.56	43.38	37.08	32.35
H2O	25.76	31.10	49.03	40.76	26.52	17.07	24.81	23.64	26.60	55.00	86.35	42.48	5.50	88.15	49.93	46.57	39.95
Ours	25.53	32.21	48.97	42.26	27.50	19.36	26.60	23.97	26.73	71.00	86.25	42.94	4.50	87.90	53.12	47.21	41.63

Table 12: Performance comparison of PyramidKV (Ours) with SnapKV (SKV), H2O, StreamingLLM (SLM) and FullKV (FKV) on LongBench for Mistral-7B-Instruct. PyramidKV generally outperforms other KV Cache compression methods across various KV Cache sizes and LLMs. The performance strengths of PyramidKV are more evident in small KV Cache sizes. Bold text represents the best performance.

Method	Single-Document QA			Multi-Document QA			Summarization			Few-shot Learning			Synthetic		Code		Avg.
	NrtvQA	Qasper	MF-en	HotpotQA	2WikiMQA	Musique	GovReport	QMSum	MultiNews	TREC	TriviaQA	SAMSum	PCount	Pre	Lcc	RB-P	
	18409	3619	4559	9151	4887	11214	8734	10614	2113	5177	8209	6258	11141	9289	1235	4206	
LlaMa-3-70B-Instruct, KV Size = Full																	
FKV	27.75	46.48	49.45	52.04	54.9	30.42	32.37	22.27	27.58	73.5	92.46	45.73	12.5	72.5	40.96	63.91	46.55
LlaMa-3-70B-Instruct, KV Size = 64																	
SKV	23.92	31.09	36.54	46.66	50.40	25.30	18.05	21.11	19.79	41.50	91.06	40.26	12.00	72.50	43.33	57.62	39.45
SLM	22.07	23.53	27.31	43.21	51.66	23.85	16.62	19.74	15.20	39.50	76.89	33.06	12.00	72.50	40.23	50.20	35.47
H2O	25.45	34.64	33.23	48.25	50.30	24.88	20.03	21.50	21.39	42.00	90.36	41.58	12.00	71.50	43.83	58.16	39.94
Ours	25.47	36.71	42.29	47.08	46.21	28.30	20.60	21.62	21.62	64.50	89.61	41.28	12.00	72.50	45.34	56.50	42.01
LlaMa-3-70B-Instruct, KV Size = 96																	
SKV	25.78	35.71	42.13	50.38	51.46	26.68	19.61	21.40	21.98	48.50	92.11	41.21	12.00	72.00	44.85	59.05	41.55
SLM	23.31	29.46	29.21	41.85	45.92	23.00	18.42	19.71	18.57	45.00	76.79	33.54	12.00	72.50	40.49	50.73	36.28
H2O	25.30	35.13	35.54	47.39	50.61	26.20	20.87	21.80	22.93	41.00	90.47	43.42	12.00	72.00	43.84	59.86	40.52
Ours	25.47	37.61	44.00	47.33	45.36	27.91	21.05	21.60	22.31	66.00	91.45	42.36	12.00	72.50	45.12	56.88	42.43
LlaMa-3-70B-Instruct, KV Size = 128																	
SKV	26.22	37.49	45.70	50.86	52.82	28.50	20.38	21.72	22.56	53.00	91.61	41.43	12.00	71.50	45.06	60.50	42.58
SLM	24.25	29.12	29.24	40.20	46.28	21.80	19.55	19.42	20.61	48.00	76.60	33.21	12.00	72.50	40.65	51.03	36.53
H2O	25.61	35.02	37.74	47.77	51.16	26.87	20.57	20.78	23.33	42.00	91.65	43.85	12.00	72.50	43.50	59.67	40.88
Ours	26.06	40.35	45.67	50.20	52.78	29.36	22.31	22.02	23.69	71.00	92.27	44.33	12.00	72.50	45.90	59.55	44.37
LlaMa-3-70B-Instruct, KV Size = 2048																	
SKV	26.73	45.18	47.91	52.00	55.24	30.48	28.76	22.35	27.31	72.50	92.38	45.58	12.00	72.50	41.52	69.27	46.36
SLM	26.69	41.01	35.97	46.55	52.98	25.71	27.81	20.81	27.16	69.00	91.55	44.02	12.00	72.00	41.44	68.73	43.96
H2O	27.67	46.51	49.54	51.49	53.85	29.97	28.57	22.79	27.53	59.00	92.63	45.94	12.00	72.50	41.39	63.90	45.33
Ours	27.22	46.19	48.72	51.62	54.56	31.11	29.76	22.50	27.27	73.50	91.88	45.47	12.00	72.50	41.36	69.12	46.55

Table 13: Performance comparison of PyramidKV (Ours) with SnapKV (SKV), H2O, StreamingLLM (SLM) and FullKV (FKV) on LongBench for LlaMa-3-70B-Instruct. PyramidKV generally outperforms other KV Cache compression methods across various KV Cache sizes and LLMs. The performance strengths of PyramidKV are more evident in small KV Cache sizes. Bold text represents the best performance.

With a small budget, our proposed method enables more effective allocation, better preserving useful attention information. Second, with a large budget, such allocation becomes less critical, as it is sufficient to cover the necessary information. To further illustrate this phenomenon, we have included an ablation study titled "Attention Recall Rate Experiment" as Figure 8. The results show that with a small budget, PyramidKV improves the attention recall rate (the percentage of attention computed using the keys retrieved by the method and the query, relative to the attention computed using all keys and the query.). However, with a larger budget (i.e., 2k KV Cache Size), the improvement decreases. For 64, 128, 256, 512, 1024 and 2048 KV Cache sizes, PyramidKV’s average attention recall rate improvements are 1.87%, 0.64%, 0.61%, 0.56%, 0.47% and 0.36%.

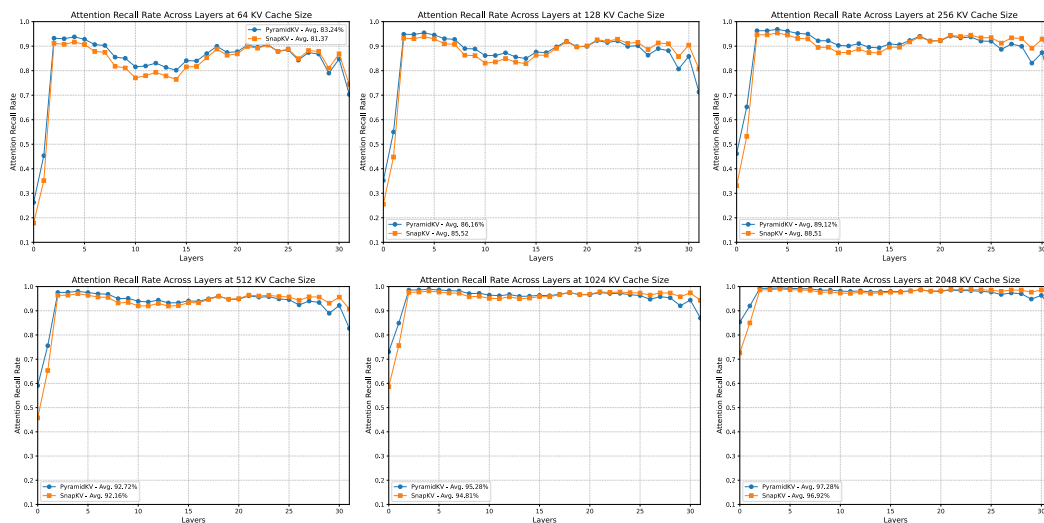


Figure 8: Attention recall rate (the percentage of attention computed using the keys retrieved by the method and the query, relative to the attention computed using all keys and the query.) comparison of PyramidKV and SnapKV.

N LONGBENCH RESULTS FOR 128 CONTEXT LENGTH

We conducted additional experiments using Llama-3-8B-Instruct-Gradient-1048k with a sequence length of 128k as Table 14. The results, summarized in the table below, showcase the model’s performance with extended context lengths. These findings provide further validation of the scalability and robustness of our approach.

Method	Single-Document QA			Multi-Document QA			Summarization			Few-shot Learning			Synthetic		Code		Avg.
	NrrvQA	Qasper	MF-en	HotpotQA	2WikiMQA	Musique	GovReport	QMSum	MultiNews	TREC	TriviaQA	SAMSum	PCount	Pre	Lcc	RB-P	
SnapKV	6.10	8.14	23.12	8.87	10.54	5.59	20.27	17.95	18.07	50.50	82.78	34.67	3.50	49.25	45.39	41.68	26.65
H2O	3.47	7.49	14.17	7.30	8.74	4.55	24.13	17.83	21.91	61.50	81.45	23.60	3.55	41.80	43.25	38.51	25.20
StreamingLLM	3.47	7.49	14.17	7.30	8.74	4.55	19.21	17.83	21.91	61.50	78.21	23.60	3.55	41.80	43.25	38.51	24.69
PyramidKV	5.41	8.42	22.61	9.71	10.73	5.82	20.37	18.24	18.32	54.00	85.33	34.60	3.50	52.75	47.23	42.58	27.48

Table 14: Comparison of PyramidKV with baselines at 128k context length.

O PYRAMIDKV PRESERVES THE LONG-CONTEXT UNDERSTANDING ABILITY

We perform Fact Retrieval Across Context Lengths (“Needle In A HayStack”) (Liu et al., 2023a; Fu et al., 2024) to test the in-context retrieval ability of LLMs after leveraging different KV cache

1350 methods. We conducted the Needle-in-a-Haystack experiment using various LLMs (i.e., Mistral-7B-
 1351 Instruct-32k, LLaMA-3-8B-Instruct-8k, and LLaMA-3-70B-Instruct-8k), various KV cache sizes
 1352 (i.e., 64, 96, and 128) and various methods (i.e., FullKV, PyramidKV, H2O and StreamingLLM).
 1353 PyramidKV achieves Acc. performance closest to FullKV, while other methods show significant
 1354 decreases. It is worth noting that PyramidKV with 128 KV cache size achieves the same 100.0 Acc.
 1355 performance compared with FullKV with 8k context size for LLaMA-3-70B-Instruct.

1356 Figure 9, Figure 10, Figure 11 show the results of **Mistral-7B-Instruct** (Jiang et al., 2023) with
 1357 different cache size (64, 96 and 128, respectively).

1358 Figure 12, Figure 13, Figure 14 show the results of **LlaMa-3-8B-Instruct** with different cache size
 1359 (64, 96 and 128, respectively).

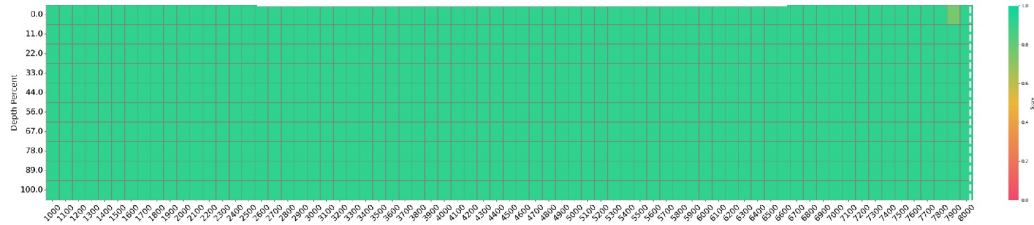
1360 Figure 15, Figure 16, Figure 17 show the results of **LlaMa-3-70B-Instruct** with different cache size
 1361 (64, 96 and 128, respectively).

1364	Model	Length	KV Cache	Full KV Acc.	PyramidKV Acc.	SnapKV Acc.	H2O Acc.
1365	Mistral-7B	32k	64	100.00	80.50	43.90	48.40
1366	Mistral-7B	32k	96	100.00	90.50	72.20	59.10
1367	Mistral-7B	32k	128	100.00	91.60	80.10	64.90
1368	LLaMa-3-8B	8k	64	100.00	92.90	62.00	31.90
1369	LLaMa-3-8B	8k	96	100.00	95.80	80.70	44.20
1370	LLaMa-3-8B	8k	128	100.00	97.40	87.40	49.10
1371	LLaMa-3-70B	8k	64	100.00	99.60	76.20	47.30
1372	LLaMa-3-70B	8k	96	100.00	98.60	94.40	69.90
1373	LLaMa-3-70B	8k	128	100.00	100.00	98.60	82.30

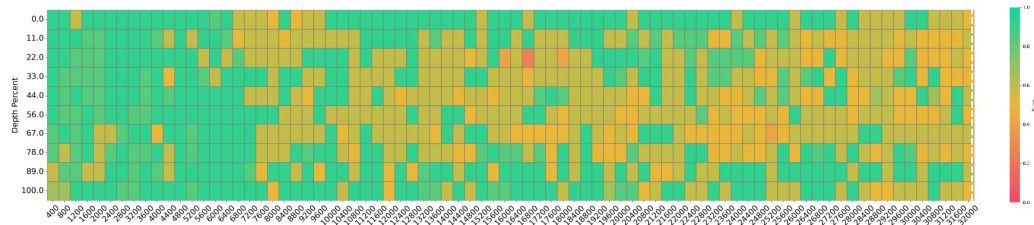
1374
 1375 Table 15: Recall Accuracy performance from Fact Retrieval Across Context Lengths (“Needle In A
 1376 HayStack”)

1404
 1405
 1406
 1407
 1408
 1409
 1410
 1411
 1412
 1413
 1414
 1415
 1416
 1417
 1418
 1419
 1420
 1421
 1422
 1423
 1424
 1425
 1426
 1427
 1428
 1429
 1430
 1431
 1432
 1433
 1434
 1435
 1436
 1437
 1438
 1439
 1440
 1441
 1442
 1443
 1444
 1445
 1446
 1447
 1448
 1449
 1450
 1451
 1452
 1453
 1454
 1455
 1456
 1457

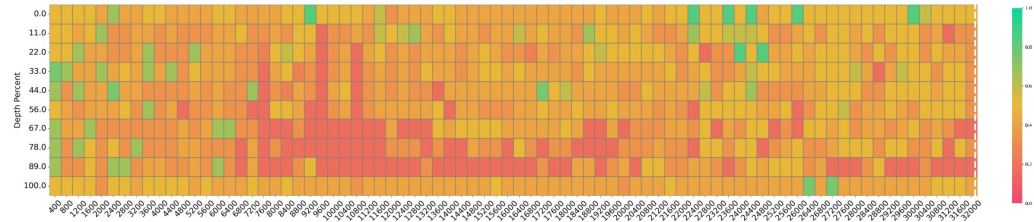
Mistral-7B-v0.2 - 32K Context Size



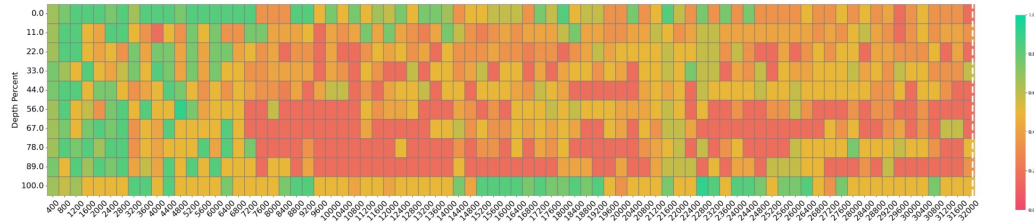
(a) FullKV, KV Size = Full, acc 100.0



(b) PyramidKV, KV Size=64, acc 80.5



(c) SnapKV, KV Size=64, acc 43.9



(d) H2O, KV Size=64, acc 48.4

Figure 9: Results of the Fact Retrieval Across Context Lengths (“Needle In A HayStack”) test in **Mistral-7B-Instruct** with **32k** context size in **64** KV cache size. The vertical axis of the table represents the depth percentage, and the horizontal axis represents the token length. PyramidKV mitigates the negative impact of KV cache compression on the long-context understanding capability of LLMs.

1458
 1459
 1460
 1461
 1462
 1463
 1464
 1465
 1466
 1467
 1468
 1469
 1470
 1471
 1472
 1473
 1474
 1475
 1476
 1477
 1478
 1479
 1480
 1481
 1482
 1483
 1484
 1485
 1486
 1487
 1488
 1489
 1490
 1491
 1492
 1493
 1494
 1495
 1496
 1497
 1498
 1499
 1500
 1501
 1502
 1503
 1504
 1505
 1506
 1507
 1508
 1509
 1510
 1511

Mistral-7B-v0.2 - 32K Context Size

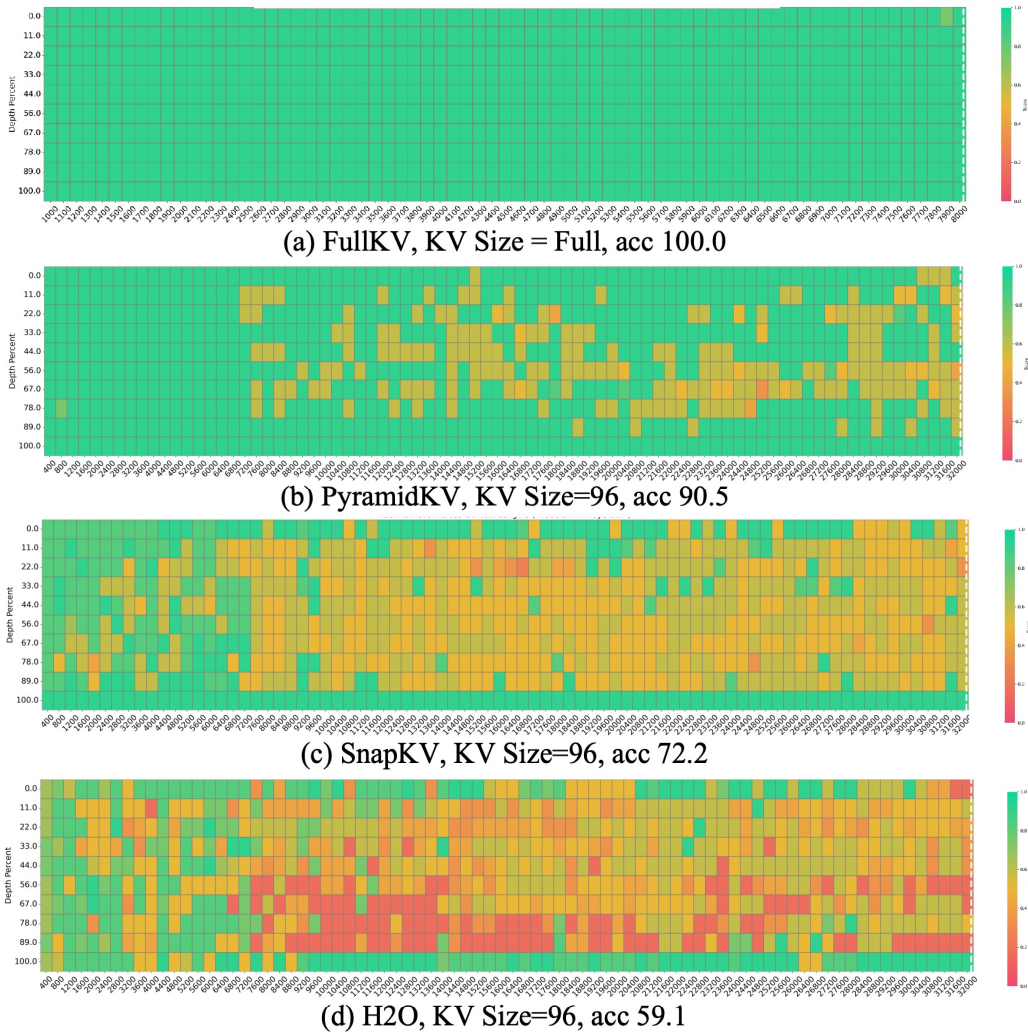


Figure 10: Results of the Fact Retrieval Across Context Lengths (“Needle In A HayStack”) test in **Mistral-7B-Instruct** with **32k** context size in **96** KV cache size. The vertical axis of the table represents the depth percentage, and the horizontal axis represents the token length. PyramidKV mitigates the negative impact of KV cache compression on the long-context understanding capability of LLMs.

1512
 1513
 1514
 1515
 1516
 1517
 1518
 1519
 1520
 1521
 1522
 1523
 1524
 1525
 1526
 1527
 1528
 1529
 1530
 1531
 1532
 1533
 1534
 1535
 1536
 1537
 1538
 1539
 1540
 1541
 1542
 1543
 1544
 1545
 1546
 1547
 1548
 1549
 1550
 1551
 1552
 1553
 1554
 1555
 1556
 1557
 1558
 1559
 1560
 1561
 1562
 1563
 1564
 1565

Mistral-7B-v0.2 - 32K Context Size

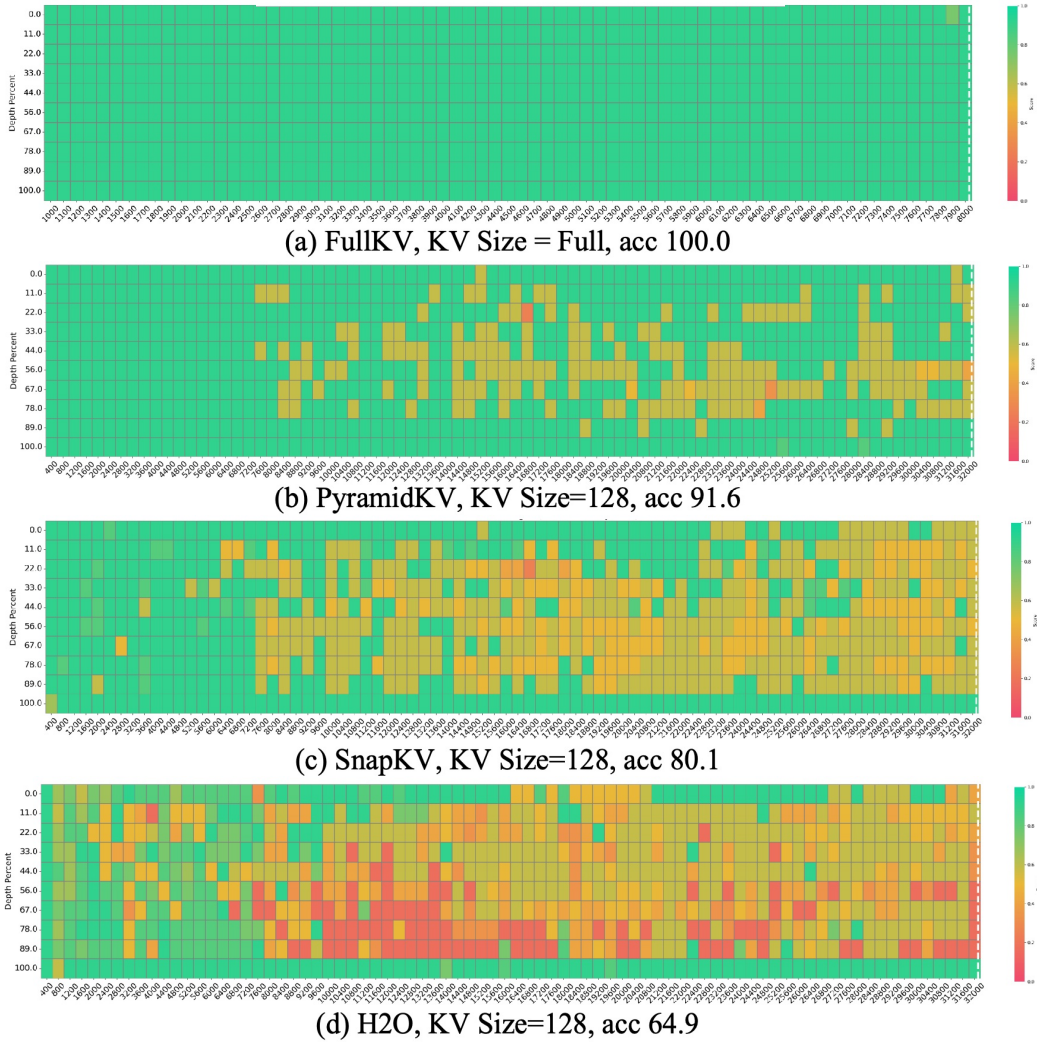
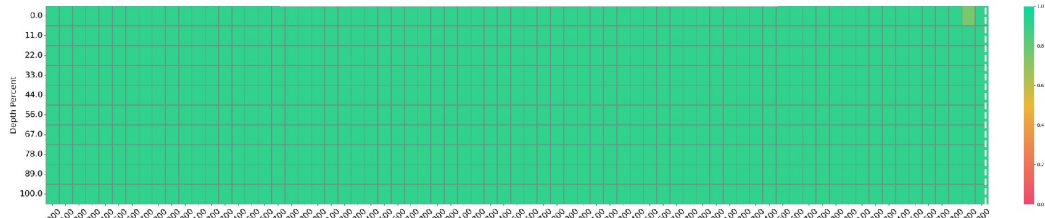


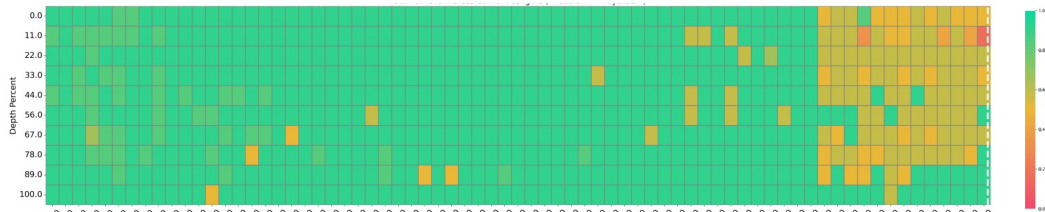
Figure 11: Results of the Fact Retrieval Across Context Lengths (“Needle In A HayStack”) test in **Mistral-7B-Instruct** with **32k** context size in **128** KV cache size. The vertical axis of the table represents the depth percentage, and the horizontal axis represents the token length. PyramidKV mitigates the negative impact of KV cache compression on the long-context understanding capability of LLMs.

1566
 1567
 1568
 1569
 1570
 1571
 1572
 1573
 1574
 1575
 1576
 1577
 1578
 1579
 1580
 1581
 1582
 1583
 1584
 1585
 1586
 1587
 1588
 1589
 1590
 1591
 1592
 1593
 1594
 1595
 1596
 1597
 1598
 1599
 1600
 1601
 1602
 1603
 1604
 1605
 1606
 1607
 1608
 1609
 1610
 1611
 1612
 1613
 1614
 1615
 1616
 1617
 1618
 1619

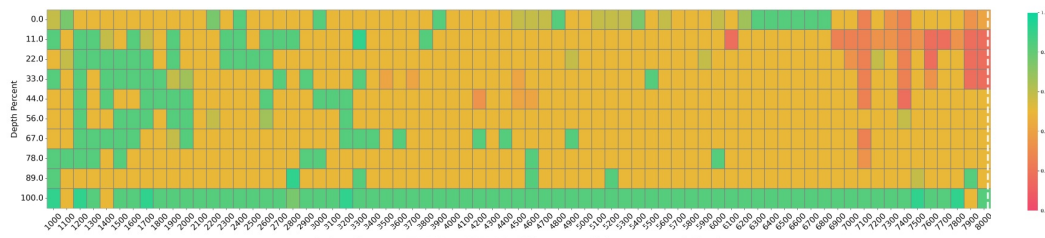
LLaMA-3-8B - 8K Context Size



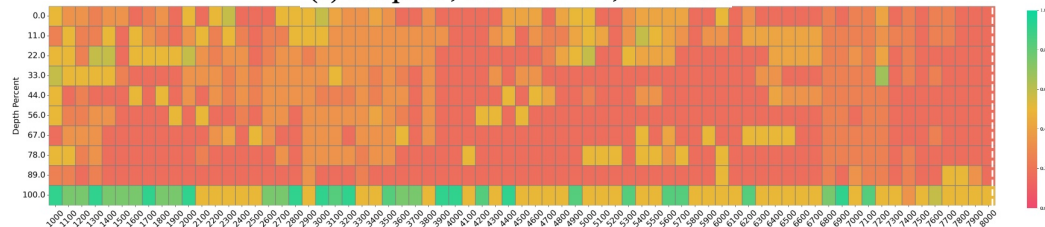
(a) FullKV, KV Size = Full, acc 100.0



(b) PyramidKV, KV Size=64, acc 92.9



(c) SnapKV, KV Size=64, acc 62.0



(d) H2O, KV Size=64, acc 31.9

Figure 12: Results of the Fact Retrieval Across Context Lengths (“Needle In A HayStack”) test in **LlMa-3-8B-Instruct** with **8k** context size in **64** KV cache size. The vertical axis of the table represents the depth percentage, and the horizontal axis represents the token length. PyramidKV mitigates the negative impact of KV cache compression on the long-context understanding capability of LLMs.

1620
1621
1622
1623
1624
1625
1626
1627
1628
1629
1630
1631
1632
1633
1634
1635
1636
1637
1638
1639
1640
1641
1642
1643
1644
1645
1646
1647
1648
1649
1650
1651
1652
1653
1654
1655
1656
1657
1658
1659
1660
1661
1662
1663
1664
1665
1666
1667
1668
1669
1670
1671
1672
1673

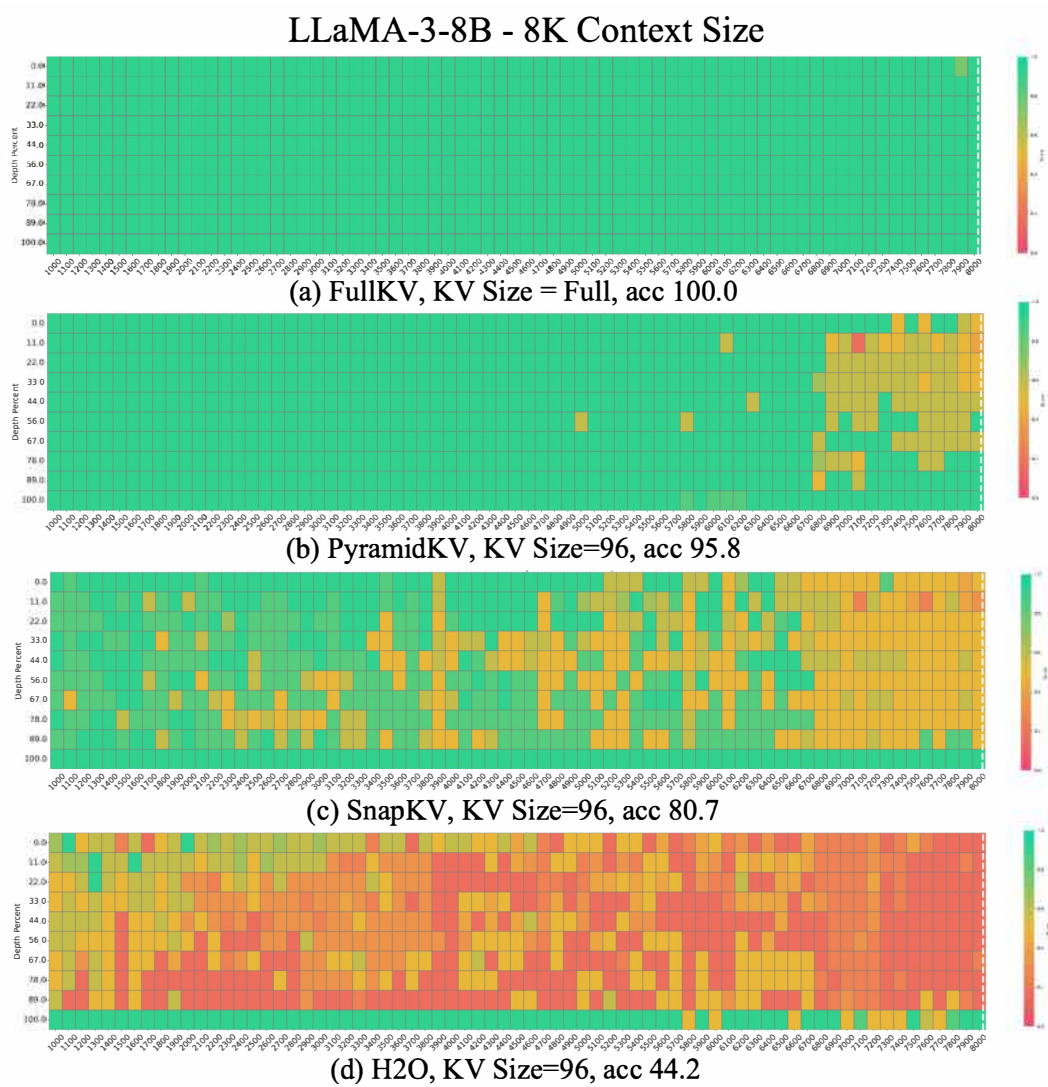
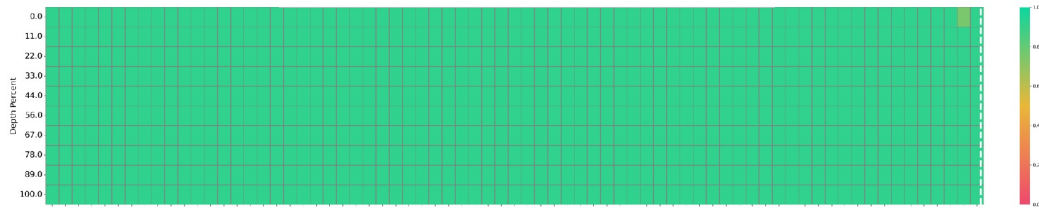


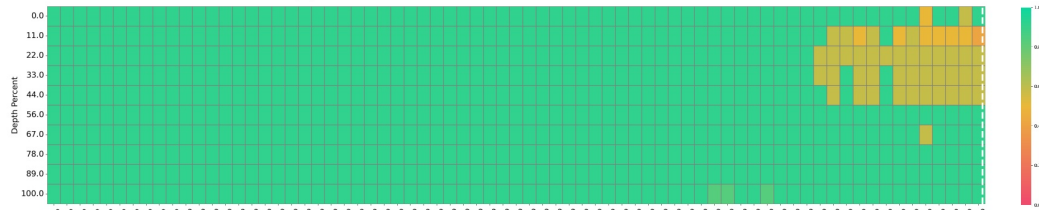
Figure 13: Results of the Fact Retrieval Across Context Lengths (“Needle In A HayStack”) test in **LlaMa-3-8B-Instruct** with **8k** context size in **96** KV cache size. The vertical axis of the table represents the depth percentage, and the horizontal axis represents the token length. PyramidKV mitigates the negative impact of KV cache compression on the long-context understanding capability of LLMs.

1674
 1675
 1676
 1677
 1678
 1679
 1680
 1681
 1682
 1683
 1684
 1685
 1686
 1687
 1688
 1689
 1690
 1691
 1692
 1693
 1694
 1695
 1696
 1697
 1698
 1699
 1700
 1701
 1702
 1703
 1704
 1705
 1706
 1707
 1708
 1709
 1710
 1711
 1712
 1713
 1714
 1715
 1716
 1717
 1718
 1719
 1720
 1721
 1722
 1723
 1724
 1725
 1726
 1727

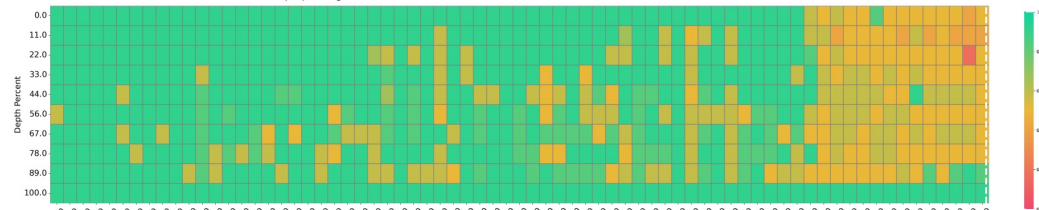
LLaMA-3-8B - 8K Context Size



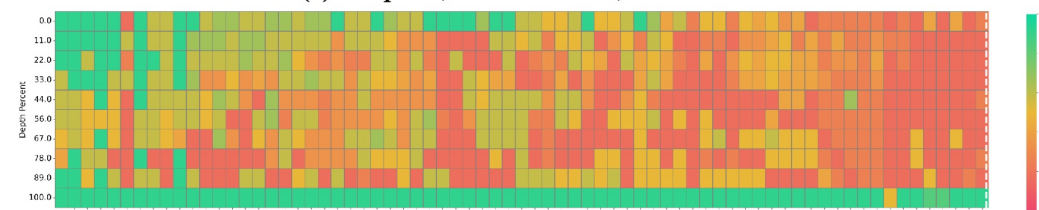
(a) FullKV, KV Size = Full, acc 100.0



(b) PyramidKV, KV Size=128, acc 97.4



(c) SnapKV, KV Size=128, acc 87.4



(d) H2O, KV Size=128, acc 49.1

Figure 14: Results of the Fact Retrieval Across Context Lengths (“Needle In A HayStack”) test in **LLaMa-3-8B-Instruct** with **8k** context size in **128** KV cache size. The vertical axis of the table represents the depth percentage, and the horizontal axis represents the token length. PyramidKV mitigates the negative impact of KV cache compression on the long-context understanding capability of LLMs.

1728
 1729
 1730
 1731
 1732
 1733
 1734
 1735
 1736
 1737
 1738
 1739
 1740
 1741
 1742
 1743
 1744
 1745
 1746
 1747
 1748
 1749
 1750
 1751
 1752
 1753
 1754
 1755
 1756
 1757
 1758
 1759
 1760
 1761
 1762
 1763
 1764
 1765
 1766
 1767
 1768
 1769
 1770
 1771
 1772
 1773
 1774
 1775
 1776
 1777
 1778
 1779
 1780
 1781

LLaMA-3-70B - 8K Context Size

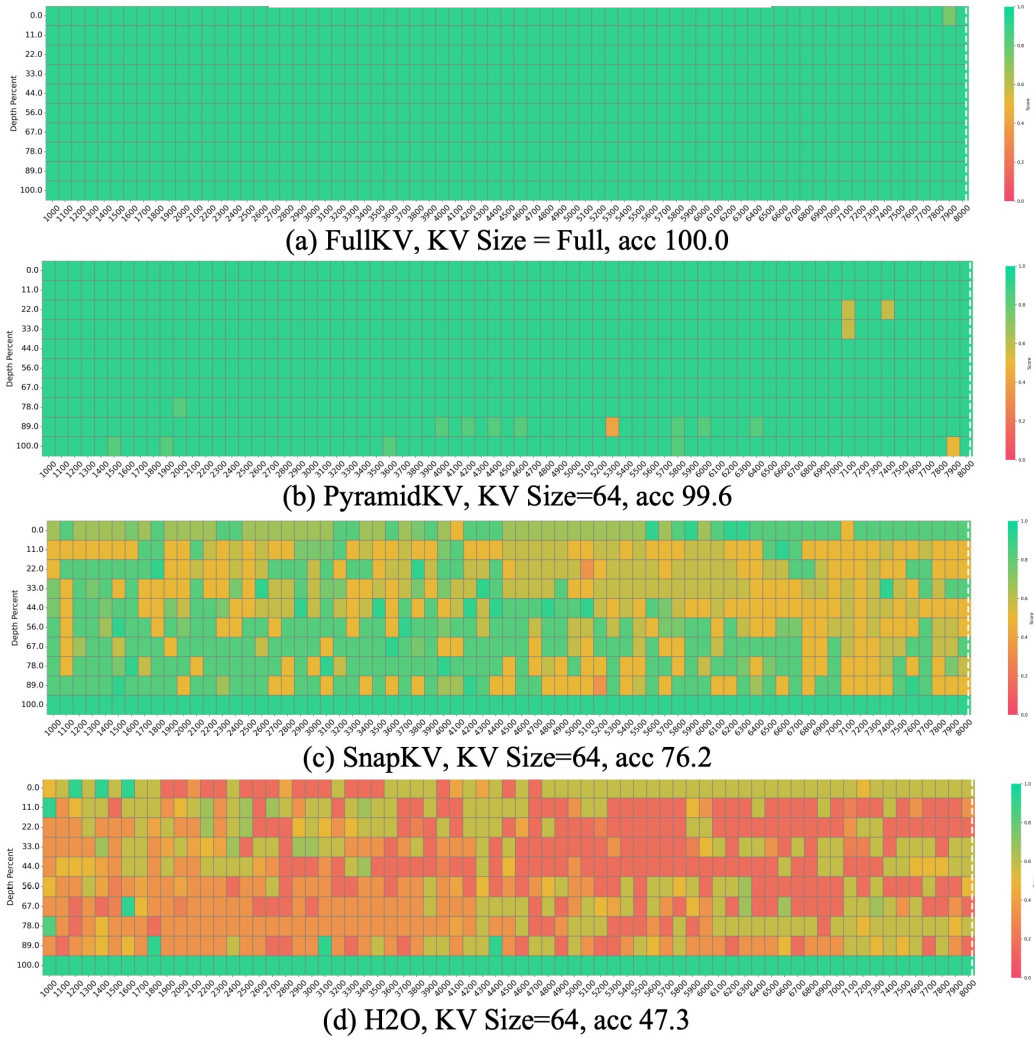
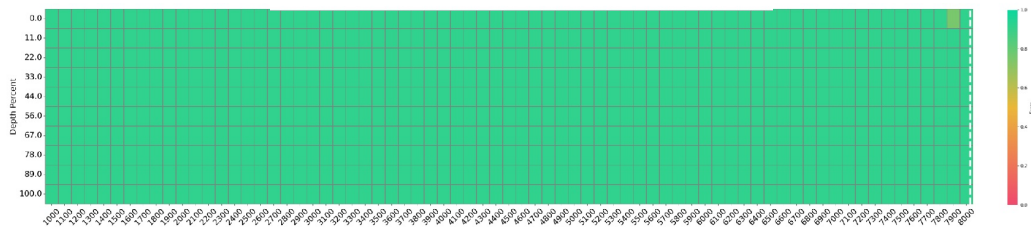


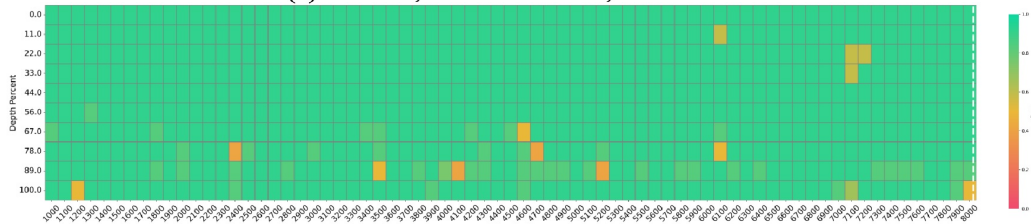
Figure 15: Results of the Fact Retrieval Across Context Lengths (“Needle In A HayStack”) test in **LlaMa-3-70B** with **8k** context size in **64** KV cache size. The vertical axis of the table represents the depth percentage, and the horizontal axis represents the token length. PyramidKV mitigates the negative impact of KV cache compression on the long-context understanding capability of LLMs.

1782
 1783
 1784
 1785
 1786
 1787
 1788
 1789
 1790
 1791
 1792
 1793
 1794
 1795
 1796
 1797
 1798
 1799
 1800
 1801
 1802
 1803
 1804
 1805
 1806
 1807
 1808
 1809
 1810
 1811
 1812
 1813
 1814
 1815
 1816
 1817
 1818
 1819
 1820
 1821
 1822
 1823
 1824
 1825
 1826
 1827
 1828
 1829
 1830
 1831
 1832
 1833
 1834
 1835

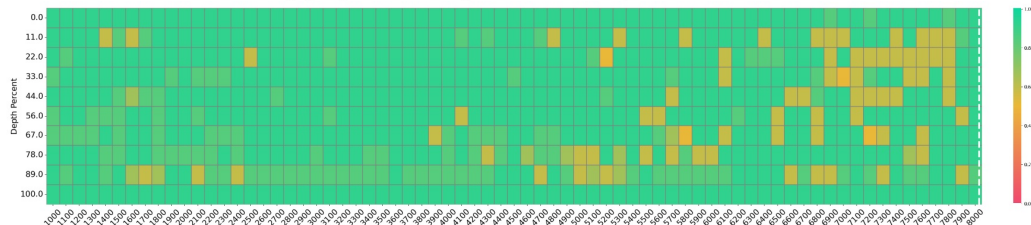
LLaMA-3-70B - 8K Context Size



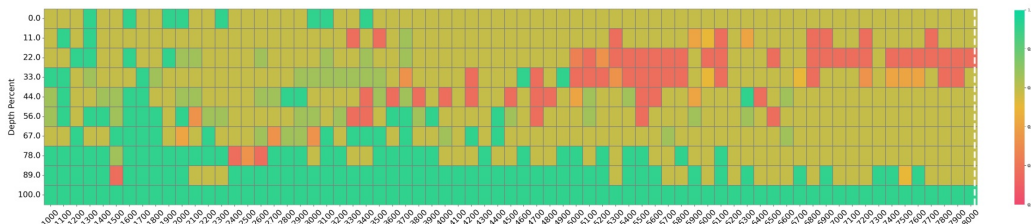
(a) FullKV, KV Size = Full, acc 100.0



(b) PyramidKV, KV Size=96, acc 98.6



(c) SnapKV, KV Size=96, acc 94.4

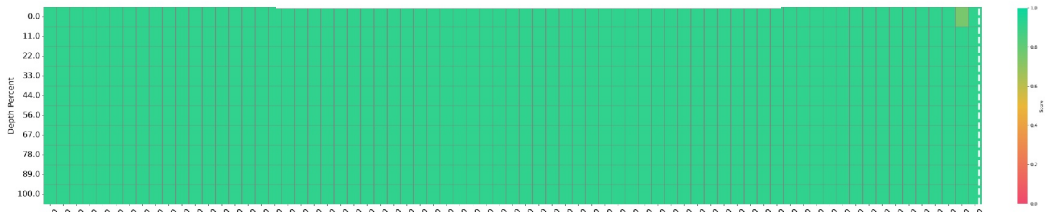


(d) H2O, KV Size=96, acc 69.9

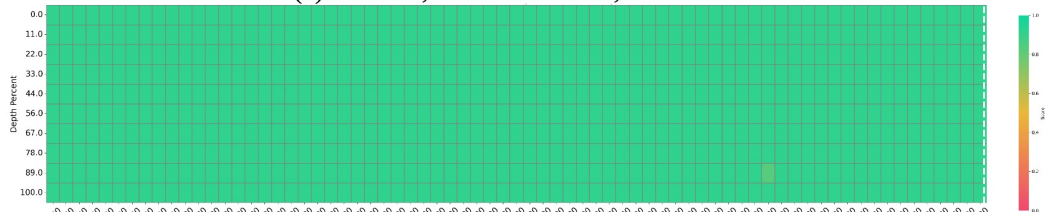
Figure 16: Results of the Fact Retrieval Across Context Lengths (“Needle In A HayStack”) test in **LLaMa-3-70B** with **8k** context size in **96** KV cache size. The vertical axis of the table represents the depth percentage, and the horizontal axis represents the token length. PyramidKV mitigates the negative impact of KV cache compression on the long-context understanding capability of LLMs.

1836
1837
1838
1839
1840
1841
1842
1843
1844
1845
1846
1847
1848
1849
1850
1851
1852
1853
1854
1855
1856
1857
1858
1859
1860
1861
1862
1863
1864
1865
1866
1867
1868
1869
1870
1871
1872
1873
1874
1875
1876
1877
1878
1879
1880
1881
1882
1883
1884
1885
1886
1887
1888
1889

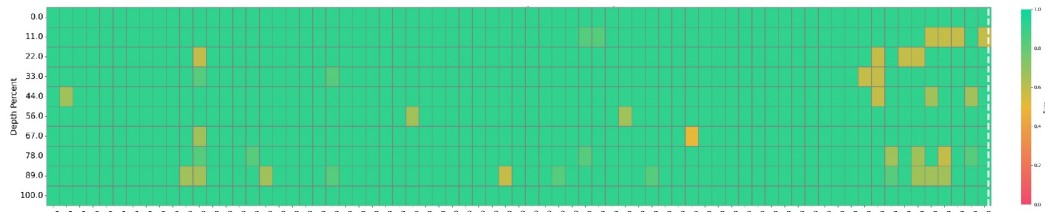
LLaMA-3-70B - 8K Context Size



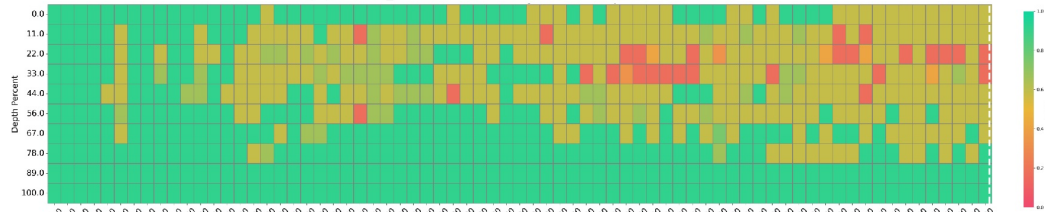
(a) FullKV, KV Size = Full, acc 100.0



(b) PyramidKV, KV Size=128, acc 100.0



(c) SnapKV, KV Size=128, acc 98.6



(d) H2O, KV Size=128, acc 82.3

Figure 17: Results of the Fact Retrieval Across Context Lengths (“Needle In A HayStack”) test in **LlMa-3-70B** with **8k** context size in **128 KV** cache size. The vertical axis of the table represents the depth percentage, and the horizontal axis represents the token length. PyramidKV mitigates the negative impact of KV cache compression on the long-context understanding capability of LLMs.

P ATTENTION PATTERNS ACROSS HEADS IN THE BOTTOM LAYER

Retrieval heads are predominantly located in the higher layers. Notably, no retrieval heads are observed in bottom layers. To further investigate, we conducted additional experiments on the bottom layer to analyze the attention patterns of the heads as Figure 18. Our findings indicate the absence of "massive attention" in any individual head.

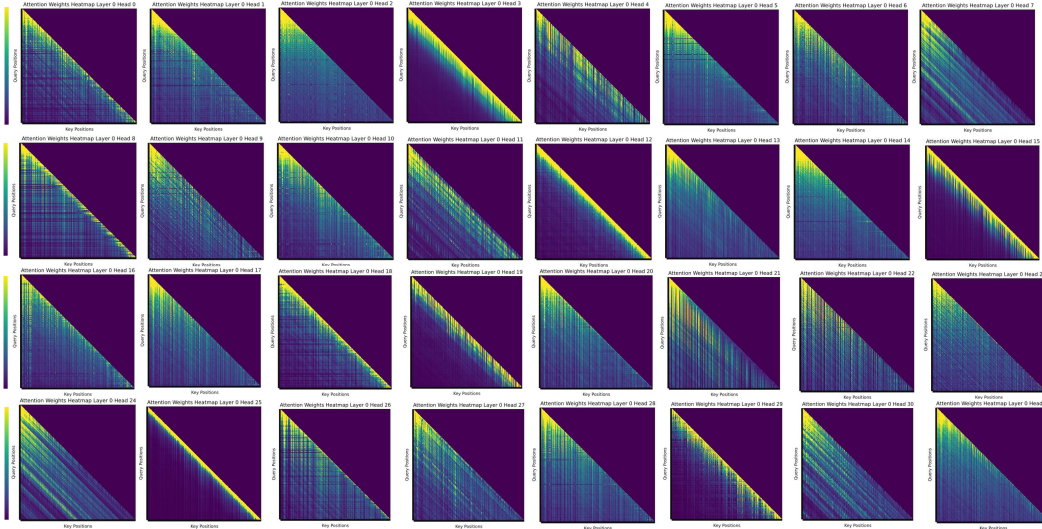


Figure 18: Attention patterns of retrieval-augmented generation across heads in the bottom layer in LLaMa.

Q PYRAMIDKV IMPLEMENTATION AT vLLM

To help compare the vLLM implementation with the vanilla dense attention backend in terms of throughput, we perform the experiment. We present the throughput comparison between the PyramidKV vLLM implementation and the vanilla dense attention backend in a setting where the inputs have varying context lengths without shared prefixes.

In Figure Figure 19, we plot the throughput of the LLaMa 8b model by varying length. We observe that relative throughput under compression decreases as the new input context length approaches the limit, causing new sequences to wait longer before being added to the decoding batch.

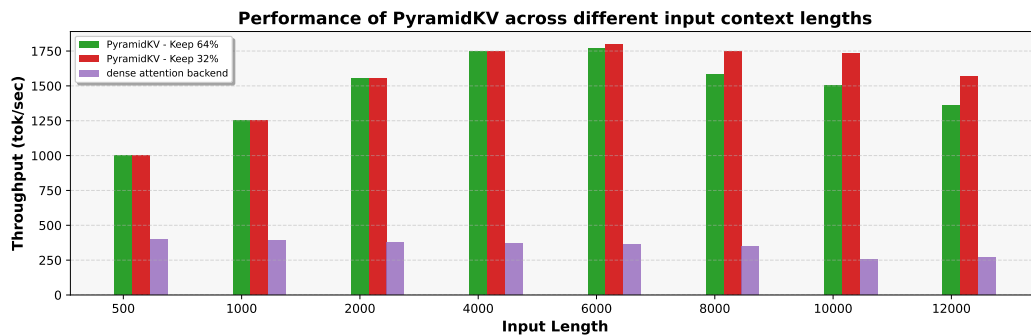


Figure 19: Throughput performance of PyramidKV across different input context lengths using LLaMa-3-8b model.

We find that allocating/releasing/moving/accessing very small chunks of memory may cause inefficiency and fragmentation in a naive implementation of PyramidKV at vLLM. As PyramidKV applies different allocation budgets for different layers. The top layers have less budget, while the bottom layers have more budget. The application of KV cache eviction with different budgets across layers at the standard paged attention frameworks (i.e., vLLM) is ineffective as it only reduces the cache size proportionally to the layer with the lowest compression rate, and all evictions beyond this rate merely increase cache fragmentation.

However, the problem could be solved by adapting paged attention to page out cache on a per-layer basis. We expand the block tables of each sequence to include block tables for each layer of the cache so that they can be retrieved for each layer’s KV cache during attention without the use of fixed memory offsets.

The implementation of PyramidKV is orthogonal to multi-gpu setting at vLLM because vLLM shards attention by head in tensor parallel, so the performance bonus would not change too much with tensor parallel or pipeline parallel. Each TP rank will have its corresponding heads of size (num_heads/tp_size). To help see the performance of PyramidKV implementation at vLLM compared with the vLLM dense attention backend at tensor parallel and pipeline parallel, we perform the experiment as Figure 20. We present the throughput comparison between PyramidKV vLLM implementation and vanilla dense attention backend at PP=1, TP=1; PP=1, TP=2; PP=1, TP=4; PP=2, TP=2 settings

Results show that the performance bonus remains similar with tensor parallel and pipeline parallel. Tensor parallelism demonstrates significant improvements when the degree is increased from 1 to 2. Notably, the result also reveals a non-linear relationship between the number of GPUs and throughput; doubling the GPU count did not yield a proportional doubling of throughput.

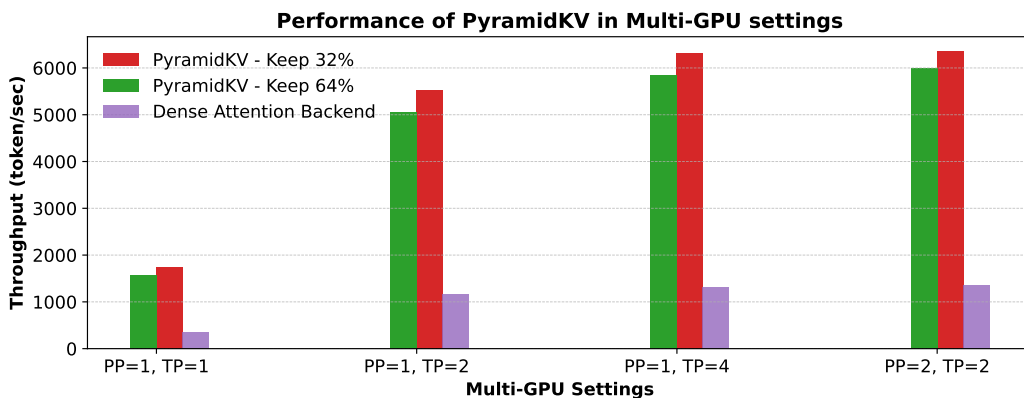


Figure 20: Throughput performance of PyramidKV across different multi-GPU settings using LLaMa-3-8b model at 8k context size.